3. Dendritic core-multishell architectures with PEI core

3.1. Introduction

The functionalization of a dendrimer or hyperbranched polar polymer with alkyl chains results in an unimolecular core-shell structure. This mimics the polarity gradient of an inverted-micelle with a polar dendritic core and a hydrophobic shell attached covalently to the core. For the first time such a system was introduced in 1996 by Stevelmans et al.[73] with PPI [G5] dendrimer used as a core. Host-guest chemistry of this and other unimolecular micelles has been evaluated, and transport phenomena of polar molecules from polar media to nonpolar solvents such as dichloromethane and toluene have been described.[19,71-73,75,80] In recent years it was proven that hyperbranched polymers such as PEI or PG functionalized with aliphatic chains are capable to encapsulate guest molecules as well as perfect dendrimers.[151,352-356,361]

The usage of unimolecular inverted micelles is unfortunately limited to nonpolar environments, and the transport of hydrophobic molecules into polar media is impossible. On the other hand, mPEG functionalized PAMAM dendrimers are able to encapsulate polar and partially nonpolar molecules in aqueous solution,[57,85] but they reveal limited stability against the pH and ionic strength change.

Systems that are based on polymeric micelles have similar limitations. It is possible to encapsulate polar guest molecules inside the inverted micelle and transport them into nonpolar environment. It is also possible to encapsulate hydrophobic guests inside the micelle and to transfer them into aqueous phase. However, encapsulation of polar and/or nonpolar molecules by one system and transport into a hydrophilic or hydrophilic environment is highly limited or impossible. The partial solution to this problem is the use of liposomes. They can encapsulate both polar and nonpolar molecules, although the use of liposomes is limited to only the aqueous media. All these described examples can be summarized as limited matrix compatibility. Therefore, the creation of an universal transport system that is suitable for various guest molecules and compatible with different environments is important and should solve many solubility and stability problems of active agents.

To achieve universal nanocompartmentation core-multishell architectures based on cheap, commercially available products have been designed. The concept of multishell architectures unites the two approaches of the unimolecular micelle and inverted unimolecular micelle into one system in which the core is surrounded by both nonpolar and polar shells. The resulting molecule can be described as the “unimolecular liposome” (Figure 19) due to mimicking of the liposome polarity gradient.

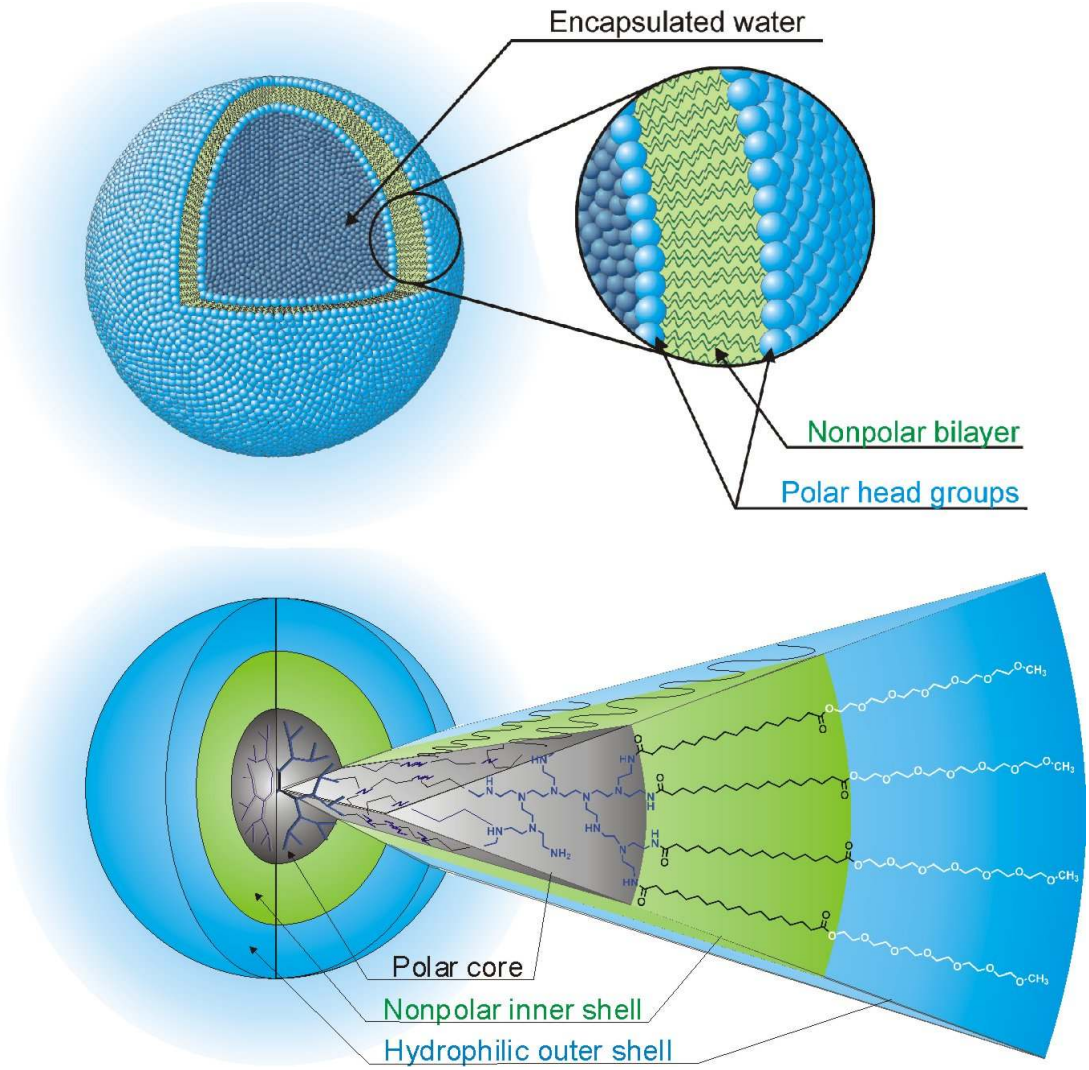

Figure 19. Schematic representation of liposome (top) and core-multishell architecture (bottom).

Based on the work presented in this thesis, only recently core-multishell architectures have been described in the literature[366] and still many questions have to be answered to fully understand dependencies, abilities, and limitations of this system. Especially the optimization of the host-guest interaction (capacity) for efficient guest uptake is necessary. In this order the influence of every building block of the polymer on the encapsulation process should be analyzed.

In this chapter the following issues will be studied:

1. Solubility of core-multishell architectures in a broad range of solvents and partition coefficient of polymers between organic and aqueous phases (chapter 3.3.)
2. Universal encapsulation abilities of polymers for polar and nonpolar guest-molecules (chapter 3.4.1.)

3. Influence of the PEI core size on the transport capacity (TC) of core-multishell architectures (chapter 3.4.2.)
4. Influence of the mPEG chain length (chapter 3.4.3.) and aliphatic chain length (chapter 3.4.4.) on the TC
5. Influence of the shell density (core functionalization level) on the TC (chapter 3.4.5.)
6. Influence of core-multishell polymer concentration on the TC (chapter 3.4.6.)
7. Dynamics of the encapsulation process (chapter 3.4.7.)

The results obtained from these experiments were the basis for further research described in chapters 4, 5, and 6.

3.2. Synthesis of core-shell architectures

In order to obtain the core-multishell architectures a three-step synthesis has been developed. The synthetic procedure was based on cheap, commercially available building blocks with the possibility of easy structural modification (Scheme 12). Hyperbranched PEI was used as a core. Linear aliphatic dicaroxylic acids were selected as an inner hydrophobic shell, and mPEGs with different molecular weights were chosen as an outer shell.

In the first step of the synthesis poly(ethylene glycol) monomethyl ether with M_w = 350, 550, 750 or 1100 g mol^{-1}, which corresponds to the chain lengths of ~6, ~10, ~14, and ~22 glycol units, respectively, is reacted with the carboxyl group of aliphatic dicarboxylic acid. The length of aliphatic chain is C_6, C_{12}, or C_{18}. The resulting amphiphilic molecules with an ester bound as a linker can be synthesized by two different methods. The first route involves water removal from the reaction mixture *via* azeotropic distillation in toluene for 18 - 48 h with a Dean-Stark trap.[367,368] The yield of the reaction is usually above 85 %. Dry *p*-toluenesulfonic acid (PTSA) or H_2SO_4 is used as a catalyst. In the second method mPEG and dicarboxylic acid are mixed and melted together in absence of solvent and catalyst. The reaction is performed with vigorous stirring under vacuum in the range of 10^{-1} to 10^{-2} mbar. The esterification process is completed after three hours with a yield in the range of 85 – 95 %. In both methods a large excess of dicarboxylic acid in comparison to the mPEG is used (3.5 to 4.0 eq.) to minimize the diesterification (diPEGylation) reaction. In the melt reaction the side-product (diPEGylated dicarboxylic acid) content ranges between 5 and 15 % and is higher than the one obtained *via* azeotropic destillation (usually 2 – 5 %). This is probably due to inefficient stirring of the reaction mixture. The problem might be overcome by using more effective methods for the mixing of the reaction. Also an increased amount of the dicarboxylic acid to 5 – 6 equivalents might reduce unwanted diPEGylation. Nevertheless, the much shorter reaction time and easy scale-up of the process make the melting route

more attractive for commercial applications. Additionally the esterification *via* azeotropic destillation with longer mPEG chains (above 2000 g mol^{-1}) requires reaction times above 48 h, which results in a partial decomposition of poly(ethylene glycol).

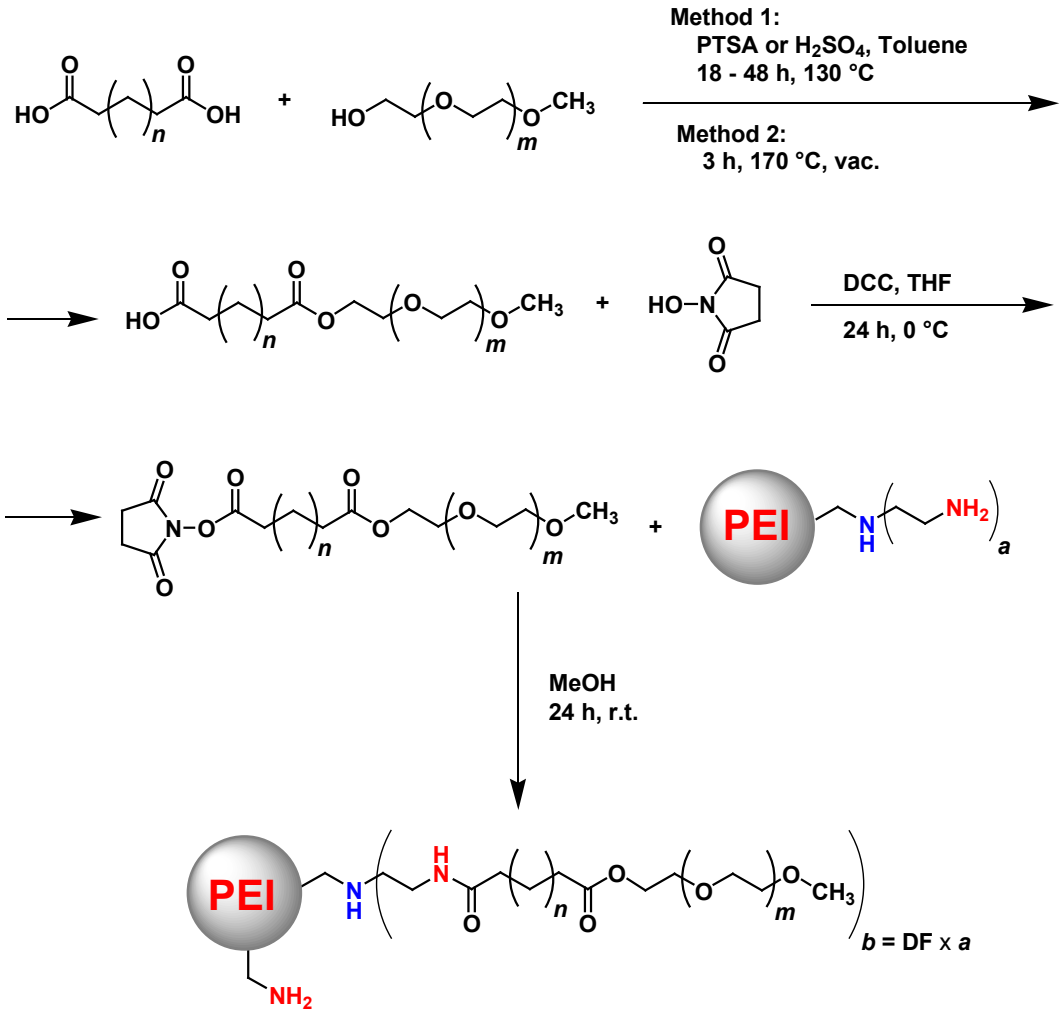

Scheme 12. Three step synthesis of core-multishell architectures with PEI core: $PEI_x(C_{n+4}mPEG_{m+1})_{DF}$; n = 2, 8, 14; $m \approx$ 5, 9, 13, 21; x = 3600, 10500; DF = 0,25 – 1,15 (DF_A = 0.10 – 0.67). In the first step the amphiphilic molecule is obtained *via* an esterification reaction. After an activation step, the amphiphile is reacted with PEI in MeOH with various molar ratios core to active ester which determine the degree of core functionalization (DF).

The reaction progress can be easily monitored by ^{1}H NMR spectroscopy (Figure 20). Creation of the ester bond shifts the signal of the mPEG protons located next to the hydroxy group from 3.63 ppm to 4.18 ppm. Therefore the conversion of reaction can be calculated by comparison of the integration values of the signals at 4.18 ppm and 3.34 ppm (mPEG's methoxy group). For the fully reacted mPEG this ratio is 2 to 3.

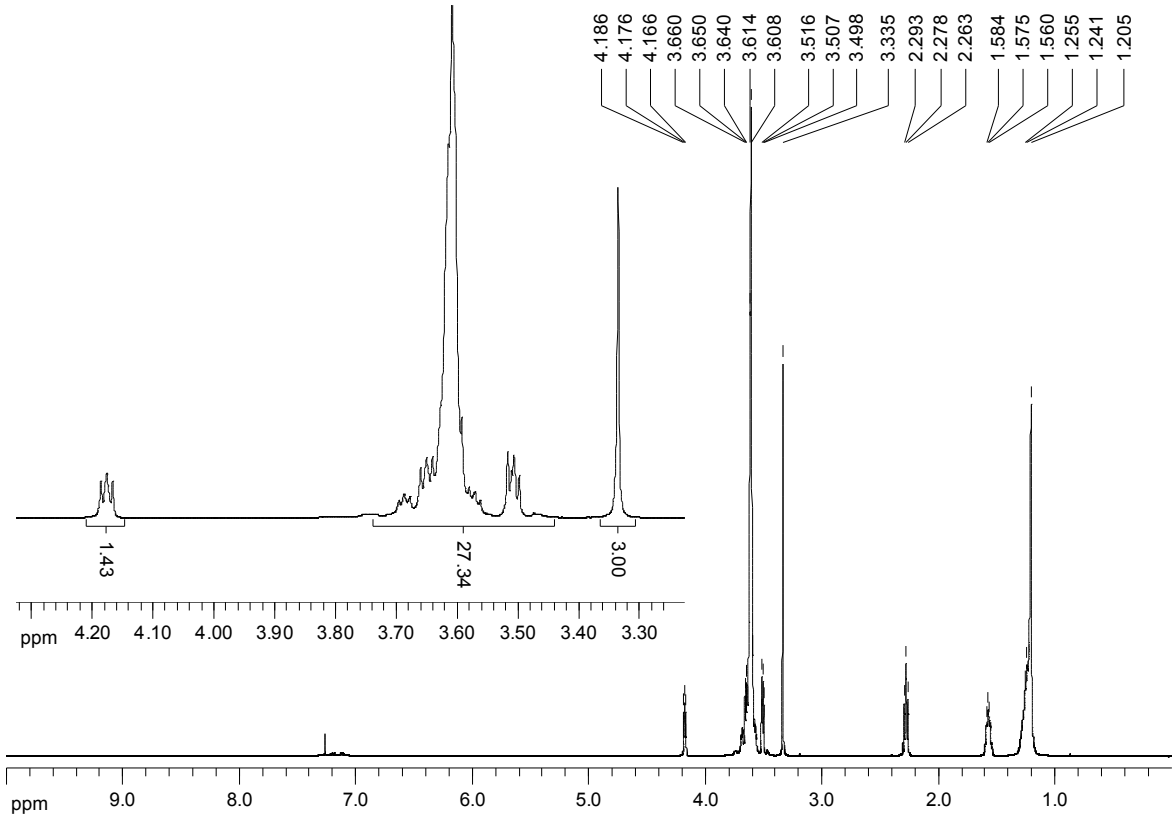

Figure 20. ^{1}H NMR spectra in $CDCl_3$ of $C_{18}mPEG_6$ ester obtained *via* azeotropic destillation after 12 h of reaction before purification. The ratio of the signal at 4.18 ppm to the signal at 3.34 ppm is 1.43 to 3.00 which corresponds to a conversion of 71.5 %.

The excess of dicarboxylic acid (C_6, C_{12} and C_{18}) can be removed by precipitation in cold (0 °C) toluene from the reaction mixture. The filtrate after removal of the solvent contains a maximum of 10 wt% of unreacted diacid in the raw product. Further purification is achieved by dry flash column chromatography. Removal of diPEGylated dicarboxylic acid is not necessary, because this side-product is unreactive and can be easily removed after the final reaction (coupling) step. The precipitated dicarboxylic acid can be washed three to four times with ethanol or methanol and drying under vacuum gives the pure starting material in amounts of 50 – 65 % calculated from the material used for the reaction. This regenerated dicarboxylic acid can be further reacted with a new portion of mPEG which was proved by repetition of the reaction up to four times without any loss of the product quality.

In the second reaction step the carboxylic group of C_ymPEG_x reacts with *N*-hydroxysuccinimide (HONSu)[369,370] in the presence of *N*,*N*'-dicyclohexylcarbodiimide (DCC).[370] As a result, the amphiphilic active ester is obtained in 96 – 99 % yield. Purification is performed by removing the crystallized 1,3-dicyclohexylurea (DCU) *via* filtration. The raw product which contains traces of DCU and HONSu is used for the following reaction without additional purification. An alternative to the HONSu activation method is 1,1'-carbonyl diimidazole (CDI).[371] CDI can be used to generate the imidazole carboxylic active ester *in*

situ which reacts selectively with primary amino groups. The disadvantage of using of the CDI activation method is the lower control over the degree of functionalization of the core and low yields in the coupling step. Additionally the core-shell polymers obtained *via* CDI coupling possess a lower purity than polymers obtained *via* HONSu reaction, even after additional dialysis.

In the final step hyperbranched PEI with different molecular weights (M_n = 3600 g mol^{-1}, PD = 1.4; M_n = 10500 g mol^{-1}, PD = 2.0) is functionalized with the activated amphiphile of the required length of hydrophobic and hydrophilic domains. As a result core-multishell architectures are obtained with a polar core, nonpolar inner shell, and polar outer shell (Scheme 12). The density of the shell depends on the degree of core functionalization (DF). This parameter describes the number of amine groups of PEI which have been converted into amides. In previous studies[361] the number of primary (T) and secondary (L) amino groups have been determined for both molecular weights of PEI used in this work. For the PEI_{3600} the number of T and L amine units are 31 and 24, respectively. PEI_{10500} possesses 76 terminal (T) and 94 linear (L) amine units (Table 1).

Table 1. Distribution of the terminal (T), linear (L), and dendritic (D) units of PEI_{3600} and PEI_{10500}.[361]

Polymer	M_w[a]	M_n[a]	M_w/M_n	DP_n	*DB*	D	L	T
PEI_{3600}	5000	3600	1.4	84	72 %	29	24	31
PEI_{10500}	21000	10500	2.0	244	62 %	74	94	76

M_w/M_n = *MWD*; DP_n – degree of polymerization - average number of monomer units per single molecule; [a] M_w and M_n are in g mol^{-1} values; D, L, and T = number of dendritic, linear, and terminal amine units per polymer.

In the case of hyperbranched poly(ethylene imine) both the L and T units may react. Since linear groups are generally located inside the core and terminal units are mostly localized on the surface of the polymer,[150,151] it was assumed that due to steric hindrance the amidation reaction mostly takes place on the terminal amino groups and only partially on linear groups. Therefore the degree of functionalization would describe the percentage of terminal groups of the core converted into amide. This value multiplied by the number of 31 or 76 for molecules with PEI_{3600} and PEI_{10500} core, respectively, gives the number of amphiphilic chains covalently connected to the center of polymer. Since linear amine groups can also react with active esters, the DF factor can be above 100%. Therefore an absolute degree of functionalization (DF_A) is introduced in this work and refers to the number of reacted units in comparison to the total number of L and T units. For example, the polymer $PEI_{10500}(C_{18}mPEG_6)_{0,9}$ has the DF of 0.9 (PEI_{10500} as a core) which gives 0.9 x 76 ≈ 68 aliphatic chains connected to the core. DF_A of this polymer is 0.4 (0.4 x 170 ≈ 68). The

degree of functionalization used in this work ranges between 0.25 – 1.20 (DF_A = 0.15 – 0.67 for PEI_{3600} and DF_A = 0.10 – 0.55 for PEI_{10500}) to determine the influence of the shell density on the stability and solubility of polymers as well as to gain insight into the theory of transport behavior. Purification of polymers was performed *via* dialysis in MeOH and/or in water with membranes of MWCO 1000 g mol^{-1} or 10000 g mol^{-1} (for more information see chapter 10.2.).

It is important to mention that additional dialyses of the polymer increase the DF factor. The observed differences between the DF before and after an additional dialysis were up to 10 %. This is due to the undesirable diffusion of the polymers from dialysis tubes. Since all polymers described in this work possess broad mass distributions, polymers with lower molecular weight diffuse faster than polymers with higher molecular weight. This results in a new mass distribution of the sample with higher M_w and therefore higher DF.

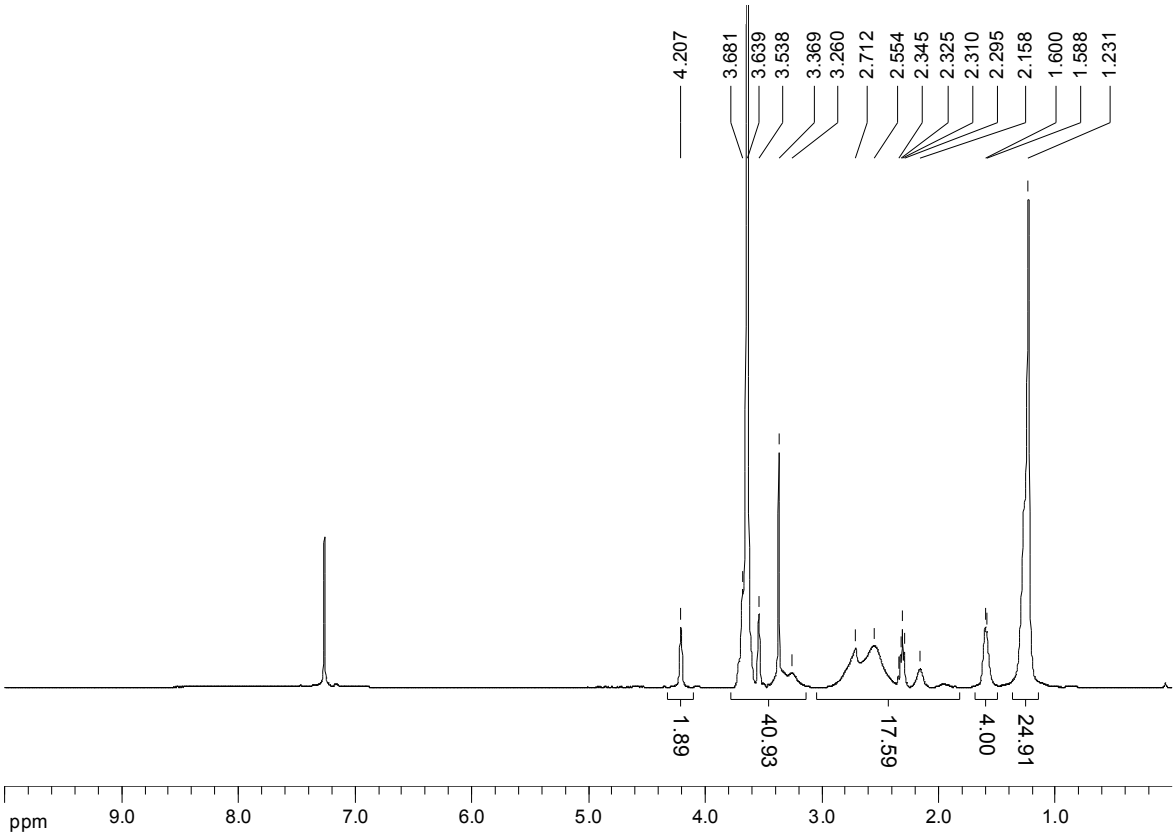

Figure 21. ^{1}H NMR spectra of $PEI_{3600}(C_{18}mPEG_6)_{0,7}$ in $CDCl_3$ (δ = 7.26 ppm) as a typical spectra of core-multishell architectures. The polymer was obtained after reaction of PEI_{3600} with $mPEG_6C_{18}ONSu$ active ester in MeOH for 24 h. The spectrum was recorded after dialysis in MeOH for 24 h. The peaks at 1.10 – 1.35 and 1.50 – 1.70 ppm derive from the aliphatic chain. The broad signal at 2.00 – 3.00 ppm belongs to the protons from the PEI core. Two peaks: triplet at 2.31 and broad signal at 2.15 ppm belong to the aliphatic chain and overlap with the PEI signal. Signals at 3.70 – 3.10 and 4.20 ppm belong to the mPEG chain and PEI protons located next to the amide bonds.

The determination of the degree of functionalization is difficult in case of the PEI based polymers and can only be calculated from ^{1}H NMR (Figure 21). A degree of functionalization obtained directly from the integration of higher functionalized polymers (above 30 %) results in an overestimation of the DF values. This is due to the shift of the signal for PEI protons located next to the amide bond from 2.00 – 3.00 ppm to 3.10 – 3.60 ppm. As a result, the integration value of the PEI signal is lower and in comparison to the integration values of the alkyl chains (range 1.10 – 1.35 ppm and 1.50 – 1.70 ppm) leads to a higher degree of functionalization than the real one. The signal of the protons on the carbons next to the amide linker overlap with the signal from the mPEG chains. Therefore, they cannot be used to determine the DF. This problem can be solved by using the iterative method of DF calculations. In general the procedure is based on multiple recalculations of the number of protons that contribute to the broad PEI signal (minus the protons from the alkyl chains equal to the value of the signal at 1.60 ppm). For unfunctionalized PEI the number of protons is equal to the DP_n value multiplied by four and this number is used as a starting point in DF_1 calculations. Since the real number of protons contributing to the signal is lower (signal intensity is lower due to amide shift), the DF_1 is higher than expected. The number of protons that are shifted to the amide range is equal to DF x T x 2 (every reacted primary group will cause the shift of the signal of two protons). When this value is subtracted from the starting value, the new number of the proton signals overlapping with the PEI signal is obtained and can be used for a new DF_2 calculation. Since the first DF was overestimated, the number of subtracted proton was also overestimated. Therefore the new DF_2 is underestimated. The next recalculation of the shifted protons based on DF_2 leads to the new DF_3, for which the value is located between DF_1 and DF_2. Two additional repetitions of the recalculation result in a degree of functionalization that is not significantly different from the previous one. Thus can be accepted as the DF value. This method has been confirmed by comparison to the DF calculated from stoichiometrical amounts of amphiphiles and PEI applied for reaction. Both results were similar and significantly different from DF obtained in the first calculation (DF_1). DFs described in this thesis are based on the presented iterative method of calculation. The calculation script is shown in the appendix.

As an alternative to the active ester coupling method a new synthetic procedure was tested to reduce the time of the complete synthesis and to allow an easy scale-up of the process. In the new method the amine groups of PEI reacted in an acid-base reaction with the carboxyl group of the corresponding amphiphile in bulk at high temperature under constant flow of inert gas. The creation of the core-multishell polymers was observed, however the reaction yield was very low. Also no control over the degree of functionalization was possible and the decomposition of the ester bond in the amphiphilic chain was noticed.

Nevertheless, due to simplicity of this reaction pathway, a further optimization of this process should result in a very efficient method of core-multishell architecture synthesis.

3.3. Stability and solubility of core-multishell architectures in various types of solvent

The terminal mPEG chains acting as an external polar layer not only provide a good biocompatibility (see chapter 1.4.) but also very good stability and solubility of the core-multishell architectures. It should be noted that the stability of the polymers was highly dependent from the DF of the molecule. Polymers with a low density of the shell and therefore a low number of mPEG chains reveal big solubility problems. After drying the core-shell structures it became very difficult to solubilize them in most of the solvents. Only after the placement of the solid polymer into polar solvents such as water, MeOH, or EtOH a very slow dissolution was observed which started with the swelling of the material. The time necessary for full dissolution depends on the composition of the polymer and the DF. This time ranged between a few days to a few months. Addition of acid into the solution reduced the dissolution time to some extent. The solubility problem is probably due to hydrophobic interactions of alkyl chains and hydrophilic interactions between the cores and the mPEGs when the self-assembly of the polymers leads to spinodal microphase separation.[372] Close contact of mPEGs and PEI cores may lead to the formation of multiple hydrogen bonds. Such highly “cross-linked” structures become hard to dissolve and only solvents which are able to distract the hydrogen bonds can dissolve the polymer again.[373] The dissolubility problem disappears for polymers with a DF value equal or greater than approximately 0.6. This value strongly depends on the size of the core and the length of aliphatic and mPEG chains and usually varies between 0.55 and 0.65 DF. In general it was observed that larger cores also cause dissolution problems at higher DF. The increase of the mPEG length allows lower functionalization levels of the polymers. Changes in the flexibility of the molecule and the better shielding of the core may have caused this phenomenon. With increasing number of amphiphilic arms covalently bound to the core, the rearrangement of the polymer geometry becomes more limited and shape of the shape become more and more the “spherical”. This reduces the interactions between the polymers only to the shell-shell ones. Core-core interactions are no longer possible, which limits the formation of the hydrogen bond between amides (Scheme 13).

Since no solubility problems were observed for substances with a DF value above 0.65, independently from the composition of the core-shell architectures, only polymers with a DF above 0.65 were chosen for further studies. Exceptions were architectures used to evaluate the influence of the degree of functionalization on the transport capacity.

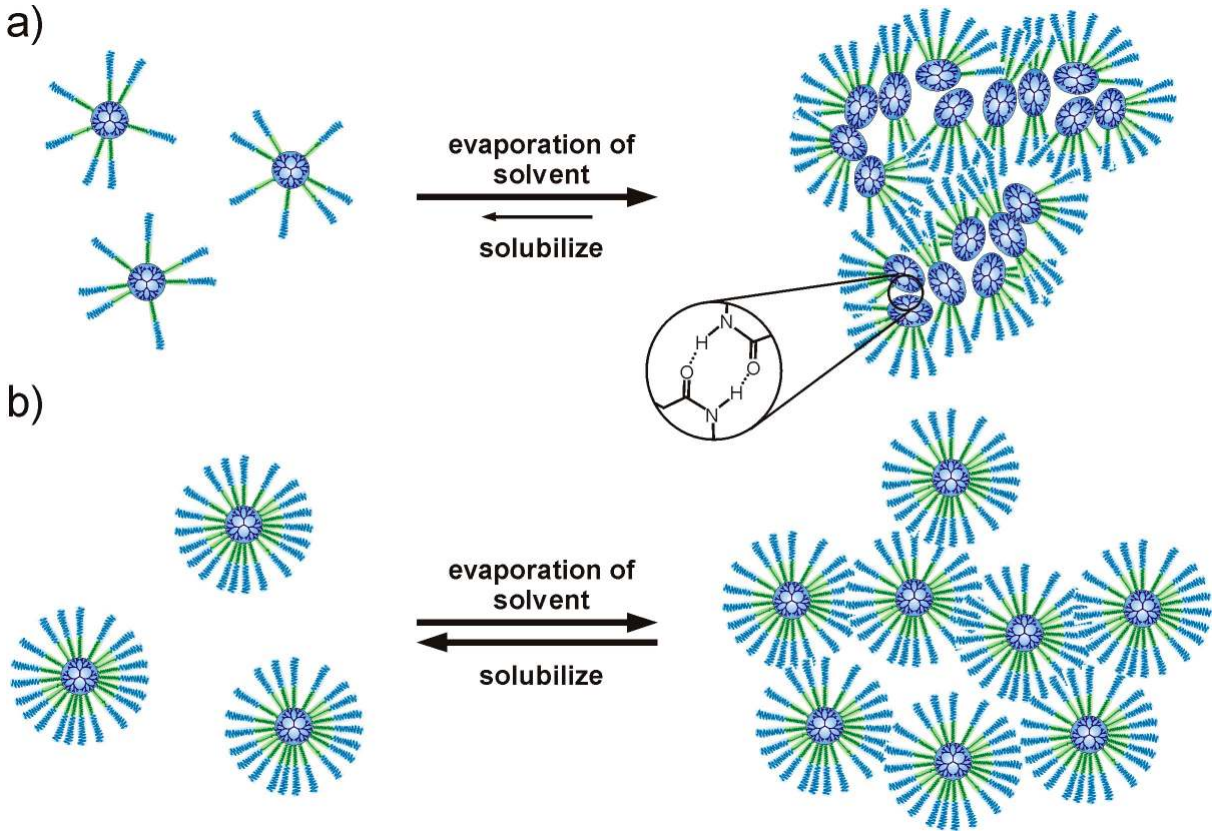

Scheme 13. Possible differences between polymer-polymer interactions for molecules with (a) DF < 0.60 and (b) DF > 0.60. For polymers with a lower degree of functionalization (a) the flexibility of the core-shell structure is bigger than for molecules with higher DF (b). Thus, reorganization of the molecule geometry and easier organization of molecules into dense patterns is possible. The interaction between molecules (hydrogen bonds) are therefore stronger than in the pattern created by dense-shell molecules where core-core interactions are not possible. The dissolution of the polymers depends on the type of the pattern and is faster for polymers with a densely surrounded core. The border between this two behaviors is usually located in the range of DF = 0.55 – 0.65 and depends on the size of the core and length of the aliphatic and mPEG chains.

Solubility of the core-multishell architectures was tested within a broad spectrum of solvents. The polarity range was varied between cyclohexane and water including such environments as toluene, chloroform, DMF, DMSO, ethanol, and methanol (Table 2). The tested polymers possess structures with both types of core (PEI_{3600} and PEI_{10500}) and mPEG chains with 6 and 14 glycol units. The length of the inner shell was limited to the C_{18} unit. DF values were chosen to be between 0.7 and 0.9. All samples revealed a very good solubility (tested concentration = 50 mg ml^{-1}) in most of the solvents tested from toluene to water, but they were completely insoluble in cyclohaxane, pentane, hexane, and diethyl ether. This solubility profile of core-multishell architecture fits to the dissolution profile of poly(ethylene glycol). Therefore we can assume that the external shell of the polymers is responsible for the interaction with the environment. The stability of the polymers in solution was tested

during three months in toluene, chloroform, ethanol, and water at r.t. No visible precipitation or color change was observed after the tests. Also the transport capacities of three-month-old samples were similar to the ones prepared from the freshly synthesized polymers. Four samples (polymers: $PEI_{3600}(C_{18}mPEG_6)_{0.7}$ and $PEI_{10500}(C_{18}mPEG_6)_{0.7}$) in chloroform and water were tested for approximately one year. None of the samples revealed any visible mark of the decomposition of the polymers. In case of $PEI_{3600}(C_{18}mPEG_6)_{0.7}$ a white precipitate in a very low amount was found at the bottom of the phial. Despite this precipitation the solution kept its host-guest properties.

Table 2. Solubility of polymers in various solvents at r.t.

Solvent	Polarity index	Solubility	Solvent	Polarity index	Solubility
water	1,000	+	DCM	0,309	+
ethylene glycol	0,790	+	chloroform	0,259	+
methanol	0,762	+	ethyl acetate	0,228	+
ethanol	0,654	+	THF	0,207	+
acetonitril	0,460	+	diethyl ether	0,117	-
DMSO	0,440	+	toluene	0,099	+
DMF	0,404	+	hexane, pentane	0,009	-
acetone	0,355	+	cyclohexane	0,006	-

+ = soluble; - = insoluble

The determination of the partition coefficient revealed an unusual behavior for core-multishell architectures. The partition coefficient (K) is described as the ratio of the solute concentration in one solvent (C_A) to the solute concentration in the second solvent (C_B) and remains constant at constant temperature (Equation 4).[374] As a very rough approximation the partition coefficient may be assumed equal to the ratio of the solubilities in the two solvents. Usually the lighter phase is defined as solvent A and the heavier phase is defined as solvent B.[375]

$$K = \frac{C_A}{C_B} = const. \qquad \text{(Equation 4)}$$

Studies were performed in two two-phase systems: water-chloroform and water-toluene. Every polymer was tested by shake-flask equilibrations [376] in two different procedures. In one method the dry sample with a precisely determined mass was first dissolved in the aqueous phase and then chloroform or toluene was added in a volume equal to the amount of water. In the second approach the dissolution of dry sample was first done in the organic phase and later mixed with the corresponding amount of water. After shaking,

the samples were stored at r.t. for 48 h. In the next step the phases were separated and solvents were removed under vacuum. The residues were weighted to determine the amounts of polymer at both phases. The experiment should lead to equal values for the partition coefficient for both described methods. This was not observed. Instead the experiment revealed that all tested polymers ($PEI_{3600}(C_{18}mPEG_6)_{0.7}$, $PEI_{3600}(C_{18}mPEG_{10})_{0.7}$, $PEI_{3600}(C_{18}mPEG_6)_{1.0}$, $PEI_{10500}(C_{18}mPEG_6)_{0.7}$, and $PEI_{10500}(C_{18}mPEG_{14})_{0.9}$) were recovered mainly from the phase in which they were initially dissolved. For example, 98 % of the $PEI_{10500}(C_{18}mPEG_6)_{0.7}$, which was dissolved in chloroform and later "incubated" with the aqueous phase, remained in the organic phase. The dissolution of the same polymer in water and following treatment with chloroform resulted in a recovery of 93 % of the core-shell architecture from the aqueous phase (Table 3). Identical experiments performed for $mPEG_6$ and $mPEG_{14}$ have shown a partition coefficient 12.0 ± 2.0 ($C_{toluene}/C_{water}$) regardless in which solvent the poly(ethylene glycol) were solubilized initially. The measurement error was ± 3 % and came from the inaccuracy of the phase separation and inaccuracy of the balance.

Table 3. Partition coefficients for core-multishell architectures obtained *via* shake-flask equilibration method.

Polymer	M_n [g mol^{-1}]	initial solvent	partition [%] in phases[a]		partition coefficient[b]
			aqueous	organic	
$PEI_{3600}(C_{18}mPEG_6)_{0.7}$	18000	H_2O	94	6	0.06
		toluene	2	98	49.0
$PEI_{3600}(C_{18}mPEG_{10})_{0.7}$	22000	H_2O	95	5	0.05
		toluene	3	97	32.3
$PEI_{3600}(C_{18}mPEG_6)_{1.0}$	24000	H_2O	93	7	0.08
		toluene	2	98	49.0
$PEI_{10500}(C_{18}mPEG_6)_{0.7}$	44000	H_2O	93	7	0.08
		toluene	2	98	49.0
$PEI_{10500}(C_{18}mPEG_6)_{0.7}$[c]	44000	H_2O	83	17	0.21
		toluene	3	97	32.3
$PEI_{10500}(C_{18}mPEG_{14})_{0.9}$	80000	H_2O	94	6	0.06
		toluene	3	97	32.3
$mPEG_6$	350	H_2O	8	92	11.5
		toluene	7	93	13.3
$mPEG_{14}$	750	H_2O	9	91	10.1
		toluene	7	93	13.3

Results obtained for chloroform used as an organic phase were similar to those obtained for toluene; [a] after 48 h incubation at 25 °C, the average error of the measurements was ±3 %; [b] $C_{toluene}/C_{water}$ ratio; [c] after 480 h of incubation at 25 °C

The obtained data lead to the suggestion that the phase-phase diffusion of this core-multishell architectures is strongly inhibited although the polymers are very good soluble in both solvents. It should be also noted that the diffusion from the aqueous into organic phase was faster than in reverse.

To explain this phenomenon the hypothesis of the nanodroplet was developed. It was assumed that during the dissolution process the polymer core and shell cavities were penetrated by solvent molecules. It is also possible that during the self-assembly of polymers into aggregates (see chapter 6) solvent molecules are incorporated in the spaces between macromolecules. Such loaded polymers behave like small, nanometer sized independent droplets of solvent and therefore become insoluble (immiscible) in another phase. The phenomenon of the swelling of the core-shell structure was observed and described by Ghosh et al.[87] In this study PAMAM based unimolecular micelles with aliphatic functions (stearyl acrylate) were used. After the addition of water to a solution of the polymer in toluene a change in the diameter was detected. The size of the macromolecules increased from 26 Å to 37 Å in diameter which was connected to an encapsulation of 480 – 580 water molecules inside the PAMAM core.

The partial diffusion of polymers after 48 h from one phase to another could be explained by a very slow exchange of solvent molecules trapped inside the polymer. This would lead to the gradual transformation of organic nanodroplets into aqueous ones and reverse. The dynamics of such transformations would determine the parameters of diffusion of the polymers between the phases. A slow transformation of the droplets would result in a very slow reaching of the equilibrium state between the phases. Thus the concentration of the polymer in both phases should change as a function of time. To confirm this theory the partition coefficient was tested for samples incubated for 48 and 480 h. Experiments performed for $PEI_{3600}(C_{18}mPEG_{10})_{0.7}$ revealed that the partition coefficient ($C_{toluene}$ /C_{water}) of core-shell architectures increases from 0.08 to 0.21 for the sample where the polymer was initially dissolved in the aqueous phase. For the sample initially solubilized in toluene the concentration in the water phase changed from 49.0 to 32.3. This would indicate that the organic phase is the preferable one for the core-multishell architectures, what is in an agreement with results obtained for pure mPEG (Table 3).

3.4. Determination of the transport capacity (TC) of core-multishell architectures

The transport capacity (TC) of core-multishell architectures can be determined in a two phase system consisting of water and chloroform or in a one phase system consisting of chloroform or water alone. Those methods can also be described as liquid-liquid extraction and solid-liquid extraction. The first procedure was described in literature as a method used

for the determination of the transport capacity of unimolecular micelles with a core based on PPI dendrimers,[73,75] PAMAM dendrimers,[350] hyperbranched PEI,[356,361] or hyperbranched PG.[355] In general this experiment was based on shaking a determined volume of a chloroform solution of core-shell structure with an equal volume of an aqueous solution of guest molecules if they were soluble in water. In the case of nonpolar guest molecules, the phase content would be reverse. The liquid-liquid extraction method possesses a high potential for TC determination for unimolecular micelles and inverted unimolecular micellar structures. Nevertheless its use for the determination of the transport capacity of core-multishell architectures is limited. Core-monoshell structures are located in just one of the phases and its concentration in solution is constant with time. The transport capacity of the core-shell structure is determined by measuring the amount of guest molecules that diffuse into the polymer containing phase. By comparing guest and polymer concentrations it is possible to calculate the average TC for a single host molecule by equation 5 where $C_{guest(total)}$ is the total concentration of the guest molecules in the solution, $C_{guest(basic)}$ is the concentration of the guest molecules in the same phase without the polymer (saturated solution), and $C_{polymer}$ is the concentration of the polymer in the tested phase.

$$TC = \frac{C_{guest(total)} - C_{guest(basic)}}{C_{polymer}} \qquad \text{(Equation 5)}$$

Due to the diffusion of core-multishell architectures from one phase into another (see chapter 3.3.) the polymer concentration in solution changes with time and cannot be precisely determined. Therefore the TC is charged with an inevitable error. Additionally the formation of highly stable emulsions during the shaking of the flask. This significantly influences the error of the measurement. Therefore solid-liquid extraction has been chosen as a standard method to determine the transport capacity of core-multishell architectures. Since the solid-liquid extraction contains only one liquid phase, some scientists argue that the obtained results should be named as a loading capacity but not as a transport capacity.[361] The dissolution of solid guest molecules is inseparably connected to the transfer of molecules from the solid phase into the liquid phase. Thus in this work both expressions describe the same.

The experiment was carried out by dissolving a precise amount of polymer in 5 ml of solvent. Water was used as a non-solvent for nonpolar molecules and chloroform as a non-solvent for polar compounds. In the next step the 10 – 20 mg of the respective drug or dye in the solid state was added to the solution and the obtained suspension was stirred vigorously (1000 rpm) for 24 h – 240 h at rt. Then the mixture was filtrated *via* 0.45 μm polytetrafluorethylene (PTFE) filters to remove any traces of insoluble residues of drug or dye

(Scheme 14). To evaluate the concentration of guest molecules in solution the UV/VIS absorption was measured and compared to the calibration curve.

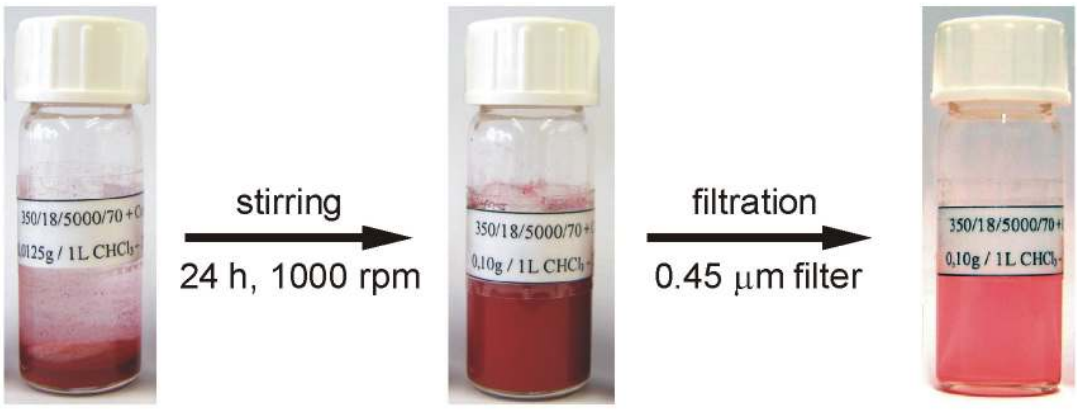

Scheme 14. Solid-liquid extraction experiment.

Due to a non-linear concentration-absorption dependency of the UV/Vis absorbance at higher concentrations of the investigated molecule, samples with an absorption above 1 AU (absorbance unit = 10 % transmittance) were diluted 5 or 10 times to avoid the significant error in TC estimation. As a reference for UV/Vis measurements the saturated solution of the investigated guest molecules in the applied solvent was used. Thus the basic solubility of dye or drug was extracted from the result. The transport capacity was calculated from equation 6 where C_{guest} is the concentration of guest molecules in solution achieved by the core-multishell architectures, and $C_{polymer}$ is the concentration of polymer in prepared solution.

$$TC = \frac{C_{guest}}{C_{polymer}} \qquad \text{(Equation 6)}$$

The TC obtained from equation 6 allows the calculation of the relative transport capacity (TC_{rel}). TC_{rel} indicates the amount of encapsulated guest molecules in grams per gram of polymer and can be calculated from equation 7 where TC is the transport capacity calculated from equation 6, M_{guest} is the molecular mass of the guest molecule, and $M_{n(polymer)}$ is the molecular mass of polymer. This value determines the encapsulation efficiency in terms of industrial usage where the crucial factor is the mass of active agent encapsulated in a standardized mass of matrix.

$$TC_{rel} = \frac{TC \times M_{guest}}{M_{n(polymer)}} \qquad \text{(Equation 7)}$$

UV/Vis calibration curves used in this work were obtained by dissolving the tested molecules in a solvent with a polarity index as close as possible to the index of the solvent used for encapsulation. The resulting solutions were diluted in series of 6 – 12 samples where the concentration of the following sample was two times lower than the concentration of the previous one (Figure 22).

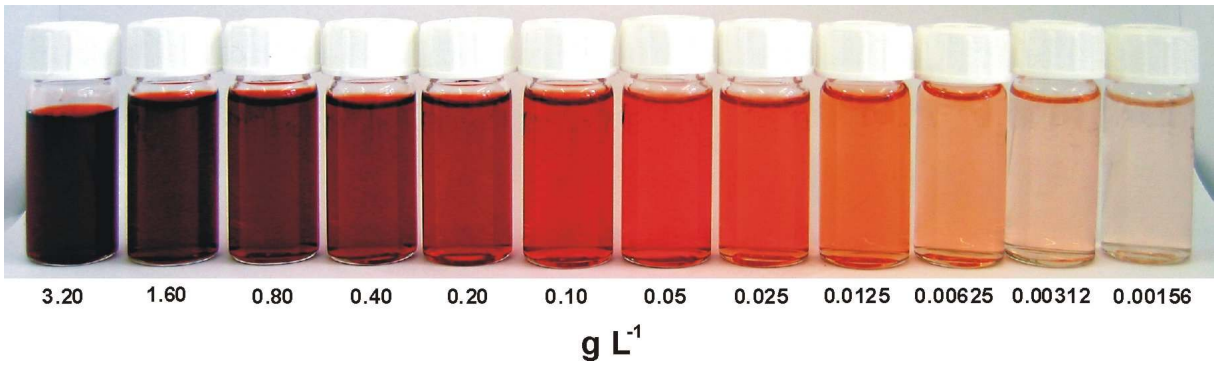

Figure 22. Congo red concentration series in water as standard for the calibration curve. The concentration of the dye decreases from left to right.

3.4.1. Universal transport abilities of nanotransporters

The versatile transport properties of dendritic multishell architectures were demonstrated by using numerous guest molecules in a wide polarity range of solvents: water, ethanol, acetone, chloroform, and toluene. In most of the tested environments the TC of individual guest molecules were similar. Thus in this work only the results obtained in water for nonpolar molecules and in chloroform for polar compounds will be described and discussed as standards. To prove the universal transport abilities of core-multishell architectures four different polar molecules and five nonpolar ones were tested by solid-liquid extraction. As examples for hydrophilic drugs and dyes *congo red* (696.7 g mol^{-1}), *rose bengal* (1049.8 g mol^{-1}), *vitamin B_6 hydrochloride – piridoxine* (205.6 g mol^{-1}), and *vitamin B_2 – riboflavin* (376.4 g mol^{-1}) were chosen (Figure 23). The guest molecule *congo red*[377] has recently been discussed as a potent neuroprotective,[378] and was used as a model compound in order to obtain results comparable to previous studies on core-shell architectures.[352,355,356,361] *Rose bengal* was used previously as a guest molecule in numerous encapsulation studies.[71-73,75,80,84] *Vitamin B_2* and *vitamin B_6* were chosen as highly important natural nutrition factors. Vitamin B_2 is responsible in humans for good vision and healthy skin, hair, and nails. It also assists in the formation of antibodies and red blood cells and aids in carbohydrate, fat, and protein metabolism.[379-381] Vitamin B_6 supports the synthesis and breakdown of amino acids as well as the metabolism of fats and carbohydrates. It additionally supports the central nervous system.[379,381]

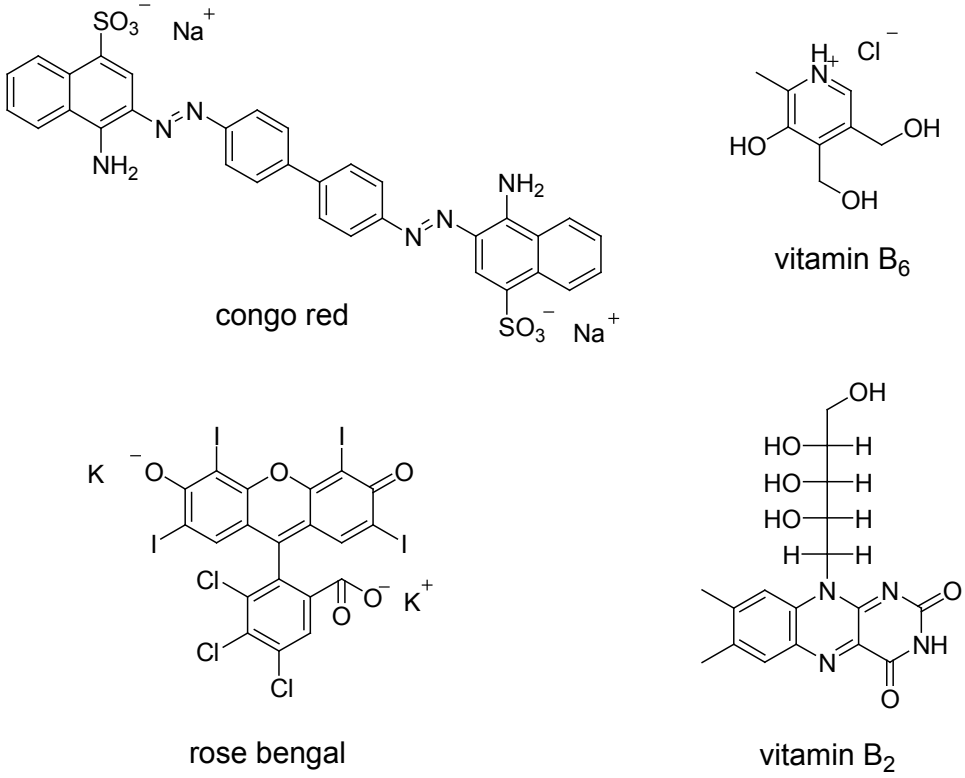

Figure 23. Structures of hydrophilic compounds used as polar guest molecules.

As representatives of hydrophobic guest molecules *β-carotene* (536.9 g mol^{-1}), *nimodipine* (Nimotop®; 418.4 g mol^{-1}), *vitamin A* (286.5 g mol^{-1}), *vitamin D$_3$* (384.6 g mol^{-1}), and *nile red* (318.4 g mol^{-1}) were used (Figure 24). *β-carotene*, which is a representative of a large group of natural hydrophobic pigments – the carotinoides, was discovered in 1831[382] and is the best known of the roughly 600 molecules in this class.[383-386] β-carotene act as a provitamin A.[384] It is also used as active compound in pharmaceuticals and cosmetics or as a coloring agent in foodstuffs and animal feeds. However, due to limited solubility of all carotinoides in fats and oils and insolubility in water, their usage is complicated.[387] β-carotene has also been considered as protective systems against oxygen radicals and singlet oxygen.[388,389] It was proven that the administration of β-carotene reduces the risk of prostate cancer.[390] The protective action of β-carotene against UV-induced skin changes has been established by Biesalski et al.[391,392] *Nimodipine* is a dihydropiridine calcium channel blocker. Nimodipine is a representative of a family of anti-tension drugs such as nifedipin (Adalat®, Cordipin®), nisoldipin, nitrendipin (Unipres®), nicardipin (Loxen®), felodipin (Pleudil®), almodipin (Norvasc®), and isradipin (Lomir®). *Nile red* is an uncharged hydrophobic phenoxazone dye whose fluorescence is strongly influenced by the polarity of its environment. It also interacts with many native proteins and shows a wide range of spectral changes for different proteins. Thus nile red is a useful probe for localizing hydrophobic domains in many proteins.[393] It also has been introduced as a fluorescent stain

for intracellular lipids.[394-397] The maximum of absorption (λ_{max}) of nile red shows a red-shift in polar solvents (564 nm in formamide) and reveals a strong blue-shift in nonpolar environments (490 nm in cyclohexane).[398] Such intensive changes in the absorption spectra allow one to use nile red as a probe to determine the location of the dye inside a core-shell structure. *Vitamin A* and *vitamin D_3* are representatives of water insoluble vitamins and are responsible for the proper function of the nervous system and absorption of calcium and phosphorus as well as for a healthy skin and nails.[379]

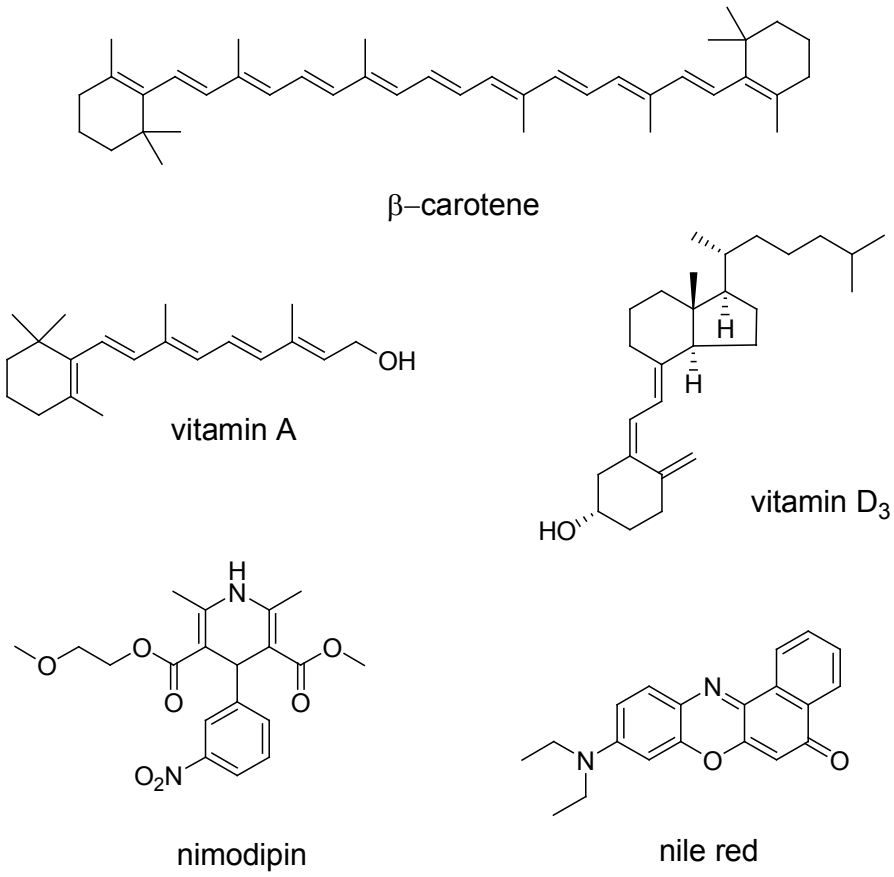

Figure 24. Structures of hydrophobic compounds used as nonpolar guest molecules.

The transport capacities for all introduced guest molecules were established. Solid-liquid extraction experiments for polar guest molecules were performed in chloroform, while the TCs of nonpolar molecules were determined in the aqueous phase. As a standard polymer $PEI_{3600}(C_{18}mPEG_6)_{0.7}$ (M_n = 18000 g mol^{-1}) was used at a concentration of 1.00 g l^{-1} (5.55 $\times$ 10^{-5} M). The results reveal universal transport abilities of the tested core-multishell architecture (Figure 25). The encapsulation of every introduced guest molecule was possible and TC_{rel} ranged between 5 – 33 mg of guest compound per g of polymer. The TC values were located between 0.15 and 1.6 guest per host molecule. In general, the transport capacities for nonpolar molecules were lower than the TCs for polar ones and lay usually

below 10 mg per g. TC_{rel} for polar compounds was usually found to be above 20 mg per g. The experimental mistakes were at maximum 20 % and were higher for nonpolar guests.

An exception was vitamin B_2 with a TC_{rel} below 5 mg per g. This might be due to the untypical character of this vitamin which is not only soluble in water but also in less polar solvents such as phenol, amyl acetate, and slightly in cyclohexanol (but is insoluble in chloroform, acetone, and diethyl ether).[399] Thus, it is possible that vitamin B_2 (due to its hydrophilic-hydrophobic character) acts as a nonpolar rather than as a polar molecule under the applied conditions. Therefore it was decided to exclude vitamin B_2 from the further experiments.

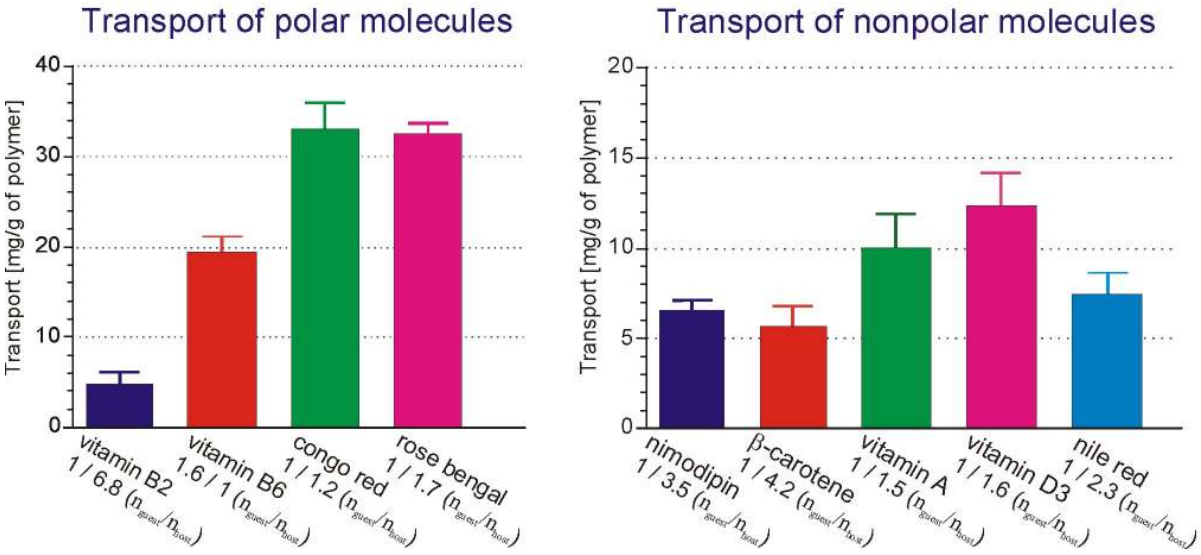

Figure 25. Transport capacities obtained with the solid-liquid extraction method for $PEI_{3600}(C_{18}mPEG_6)_{0,7}$ (concentration of polymer = 1.00 g l^{-1}). Measurements for polar molecules were performed in chloroform and for nonpolar guest molecules in water at pH 7.0.

It can be assumed that the differences between the transport abilities of polar and nonpolar molecules result from dissimilar mechanisms of encapsulation. To fully understand the mechanisms of the host-guest phenomena and its dependency from the polymer structure, systematic studies on the transport-structure relationship were performed and described in chapters 3.4.2. – 3.4.7.

Additionally, encapsulation results obtained for congo red and rose bengal revealed enormous differences between the transport capacities of core-multishell architectures and inverse unimolecular micelles described in the literature.[75,356,361] Core-shell systems based on PPI dendrimers[75] and hyperbranched PEI[361] were reported to possess encapsulation capacity in the range of 50 to even 100 dye molecules per single host molecule. The TC of $PEI_{3600}(C_{18}mPEG_6)_{0.7}$ for congo red and rose bengal was approximately 100 times lower and

lay in the range of 0.87 molecules of congo red per polymer molecule. The dissimilar encapsulation procedure used in TC measurements may explain the obtained differences in the loading capacities. Results with high TCs were obtained with the liquid-liquid extraction method while the TCs for multishell structures were obtained *via* solid-liquid extraction. The TC values reported in literature for the unimolecular micelles with dendritic PPI core achieved by solid-liquid extraction were significantly lower. A maximum of seven molecules of rose bengal were trapped in the host molecule.[73] Also solid-liquid extraction experiments performed for inverted unimolecular micelles with PEI core revealed TCs below one for all tested polymers.[361] To confirm the influence of the encapsulation method on the polymer host-guest capacity the comparison test was performed for $PEI_{10500}(C_{18}PEG_6)_{0.7}$. Solid-liquid extraction revealed a transport capacity of 4.8 while liquid-liquid extraction led to a ratio of 14.7 (n_{guest} / n_{host}) (Figure 26). The encapsulation ratio increased therefore by a factor of 2.8. The TC value was obtained by chloroform-water phase separation and UV/Vis measurement. It can be concluded that water enhances the uptake of hydrophilic guest molecules. It was also discussed in the literature that significant amounts of water were encapsulated in polyamine core and improved the phase transport properties.[76,87] Further studies revealed that differences of the transport capacities obtained by these two methods (solid-liquid and liquid-liquid) depend on the phase transfer dynamics and will be discussed in chapter 3.4.7.

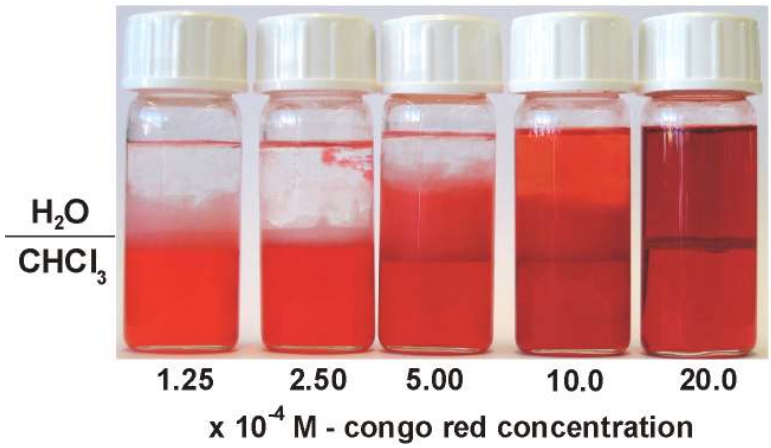

Figure 26. Liquid-liquid extraction method for transport capacity measurement for $PEI_{10500}(C_{18}mPEG_6)_{0.7}$ at a concentration of 2.00 g l^{-1} (4.55×10^{-5} M). Core-shell architecture was dissolved in 4 ml of chloroform and 4 ml of solution of congo red in water was added. Samples were shaken for 30 sec and left for phase separation for 72 h at r.t. and then the photo of phials was taken. The concentration of congo red increases from left to right. Up to concentration of congo red of 5.0×10^{-4} M the transfer of dye from the aqueous into the organic phase is quantitative. The UV/Vis measurements were performed for samples with 10.0×10^{-4} M and 20.0×10^{-4} M initial congo red concentration.

3.4.2. Dependence of the TC on the molecular weight of PEI core

Previous studies revealed that the encapsulation abilities of polymer for polar guests are directly connected to the core size of the core-shell architecture.[87,361] Increasing the core size resulted in the enhancement of the transport capacity for hydrophilic compounds.

In order to determine the influence of the M_n of the polymer core on the TC of core-multishell architectures two different PEIs with M_n = 3600 g mol^{-1} and M_n = 10500 g mol^{-1} were functionalized with amphiphilic shell *via N*-hydroxysuccinimide activation reaction route and purified by dialysis in MeOH for 24 h. For comparison $PEI_{3600}(C_{18}mPEG_6)_{0.7}$ and $PEI_{10500}(C_{18}mPEG_6)_{0.7}$ were chosen. Both polymers possess an identical exterior with C_{18} aliphatic inner shell and $mPEG_6$ as the outer, hydrophilic shell. The degree of functionalization for both nanotransporters was determined by ^{1}H NMR to be 0.7. The DF_A values were 0.40 and 0.32 for the polymers with PEI_{3600} and PEI_{10500} as a core, respectively. Transport capacities were tested by solid-liquid extraction. The polymer concentration was 1.00 g l^{-1} (5.55 $\times$ 10^{-5} M for $PEI_{3600}(C_{18}mPEG_6)_{0.7}$ and 2.27 $\times$ 10^{-5} M for $PEI_{10500}(C_{18}mPEG_6)_{0.7}$). As solvents chloroform was used for polar and water for nonpolar guest molecules. For comparison of the transport capacities for polar and nonpolar molecules congo red and β-carotene were chosen as representatives of relatively large and linearly shaped molecules. Vitamin B_6 and nimodipine were chosen as examples of compact guests. Obtained values revealed the expected increase of the TC for both polar and nonpolar compounds with increasing core size (Table 4; Figure 27). Although the increase of TC for hydrophilic molecules was significant with the factor 5.5 for congo red and 6.4 for vitamin B_6, the changes of the encapsulation capacity for hydrophobic guests were less intensive. The TC grew only by a factor of 2.1 for both β-carotene and nimodipine. Taking the growth of the molecular weight of from 18000 to 44000 g mol^{-1} (factor 2.4) into account, the relative transport capacity (TC_{rel}) for nonpolar guests slightly decreased in mg per g ratio with increasing core size. The TC_{rel} for congo red and vitamin B_6 improved significantly at the same time and were approx. 2.5 times higher for the polymer with the bigger core.

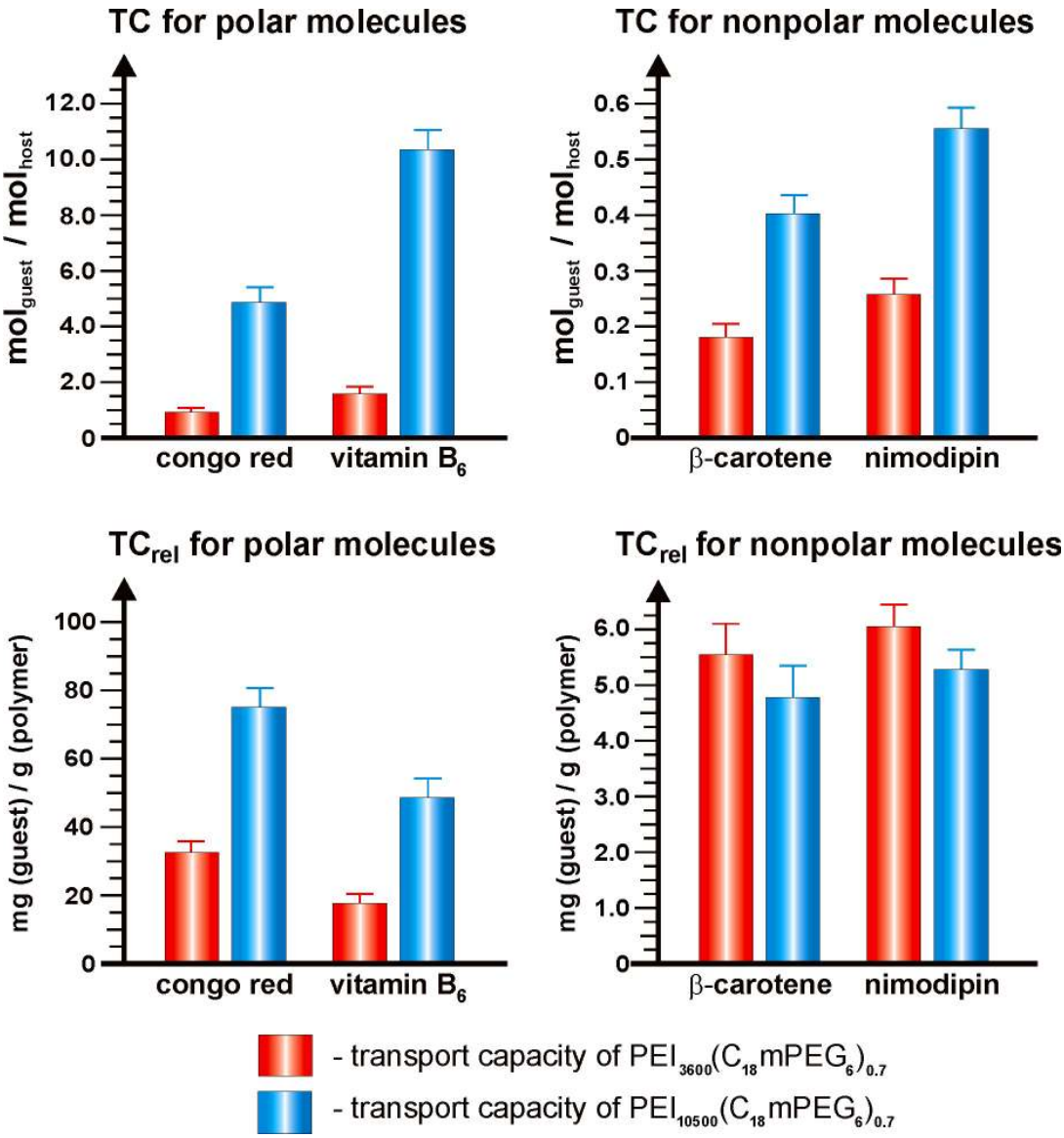

Figure 27. Influence of the core size (PEI_{3600} (red) and PEI_{10500} (blue)) on the transport capacity of core-multishell architectures. The transport dependency of polar (right) and nonpolar (left) guest molecules is presented in mol_{guest} / mol_{host} (TC) (upper) and mg (guest) per g (polymer) (bottom) ratios. Numeric data are shown in Table 4.

Table 4. Transport capacities and TC_{rel} for congo red, vitamin B_6, β-carotene, and nimodipine of $PEI_x(C_{18}mPEG_6)_{0.7}$ polymers with x = 3600 and 10500 g mol^{-1}.

Polymer	M_n [g mol^{-1}]	M_n (PEI) [g mol^{-1}]	Guest molecule	TC [C_g/C_h]	TC_{rel} [mg/g]
$PEI_{3600}(C_{18}mPEG_6)_{0.7}$	18000	3600	congo red	0.87	33.73
			vitamin B_6	1.61	18.35
			β-carotene	0.19	5.62
			nimodipine	0.26	6.06
$PEI_{10500}(C_{18}mPEG_6)_{0.7}$	44000	10500	congo red	4.81	76.06
			vitamin B_6	10.32	48.18
			β-carotene	0.40	4.88
			nimodipine	0.55	5.26

Concentration of polymer 5.55×10^{-5} M (1.00 g l^{-1}) for x = 3600 g mol^{-1} and 2.27×10^{-5} M (1.00 g l^{-1}) for x = 10500 g mol^{-1}; M_n = molecular weight of polymer calculated from ^{1}H NMR; M_n (PEI) = molecular weight of the PEI core; TC = mol_{guest} / $mol_{host} \equiv C_{guest}$ / $C_{polymer}$; TC error is ~10 %; TC_{rel} = mg of guest molecules per g polymer.

Experiments performed with $PEI_x(C_{12}mPEG_6)_{0.9}$ and $PEI_x(C_{18}mPEG_{14})_{1.0}$ polymers series (x = 3600 or 10500 g mol^{-1}) revealed a similar tendency for the transport capacities (Table 5). In every case the transport of polar and nonpolar molecules increased with the growth of the core size. The most significant change was observed for $PEI_x(C_{18}mPEG_{14})_{1.0}$ polymers where TC for congo red increased by a factor of 4.75. An exception was the encapsulation of β-carotene by polymers $PEI_x(C_{12}mPEG_6)_{0.9}$ where TC stayed nearly identical for core-multishell architectures with different core size. The relative transport capacities increased only for the polar guest molecules. For nonpolar molecules TC_{rel} decreased in all cases by a minimum factor of 2.2.

Table 5. Transport capacities and TC_{rel} of congo red and β-carotene for $PEI_x(C_{12}mPEG_6)_{0.9}$ and $PEI_x(C_{18}mPEG_{14})_{1.0}$ polymers with x = 3600 and 10500 g mol^{-1}.

Polymer	M_n [g mol^{-1}]	M_n (PEI) [g mol^{-1}]	Guest molecule	TC [C_g/C_h]	TC_{rel} [mg/g]
$PEI_{3600}(C_{12}mPEG_6)_{0.9}$	19000	3600	congo red	0.94	34.44
			β-carotene	0.22	6.17
$PEI_{10500}(C_{12}mPEG_6)_{0.9}$	48500	10500	congo red	2.55	36.58
			β-carotene	0.21	2.29
$PEI_{3600}(C_{18}mPEG_{14})_{1.0}$	36500	3600	congo red	1.13	21.52
			β-carotene	0.57	8.32
$PEI_{10500}(C_{18}mPEG_{14})_{1.0}$	95000	10500	congo red	5.37	39.39
			β-carotene	0.66	3.74

Concentration of polymer was 1.00 g l^{-1} in all experiments; M_n = molecular weight of polymer calculated from ^{1}H NMR; M_n (PEI) = molecular weight of the PEI core; TC = mol_{guest} / mol_{host} ≡ C_{guest} / $C_{polymer}$; TC error is ~10 %; TC_{rel} = mg of guest molecules per g polymer.

In conclusion, polymers with PEI cores of higher molecular weight are able to encapsulate more guest molecules irrespective of the guests' polarity. The increase of the transport capacity is more significant for polar than for nonpolar molecules. This tendency is independent from the degree of functionalization of the polymers as well as from the composition of the shell. Nevertheless, the quantitative change in the TC is strongly dependent upon both DF and shell composition. The biggest changes were observed for polymers with a low degree of functionalization and small mPEG domain while the smallest changes were detected for polymers with a short inner shell (C_{12}). The changes in TC_{rel} are significantly different from the changes of the TC values. In the case of nonpolar dyes/drugs the growth of the number of encapsulated guest molecules inside a single polymer cannot compensate for the decreasing number of polymer molecules in one gram of substance. This is due to an appreciable increase of the molecular weight of the polymer with the enlargement of the core. Thus the TC_{rel} for nonpolar guest molecules decreases for every tested polymer with increasing M_n of PEI. The experiments with polar guests revealed that the growth of the polymer molecular weight does not disturb the increase of TC_{rel}. The loading capacity for nanotransporters with PEI_{10500} is always higher than for polymers with PEI_{3600} core due to the faster growth of TC compared to the change of M_n of the polymer.

In general, the increase of the core size in the gram per gram ratio is highly profitable for the encapsulation of polar molecules but is unfavorable for the transport of nonpolar molecules. Thus from the practical (commercial) point of view the core-multishell architectures with the smaller PEI core should be applied for the encapsulation of nonpolar molecules, while polymers with bigger core should be used as nanotransporters for polar active agents.

3.4.3. Dependence of the TC on the length of mPEG chain

The influence of the poly(ethylene glycol) chain length on the transport capacity was tested with two series of polymers. The first one with PEI_{3600} (M_n = 3600 g mol^{-1}) as a core and with a degree of functionalization of 0.7 (DF_A = 0.4). As a hydrophilic shell $mPEG_6$, $mPEG_{10}$, and $mPEG_{14}$ were chosen [polymers: $PEI_{3600}(C_{18}mPEG_6)_{0.7}$, $PEI_{3600}(C_{18}mPEG_{10})_{0.7}$, and $PEI_{3600}(C_{18}mPEG_{14})_{0.7}$]. The second series based on PEI_{10500} as a core (M_n = 10500 g mol^{-1}) with a DF of 1.0 (DF_A = 0.45). $mPEG_6$, $mPEG_{10}$, $mPEG_{14}$, and $mPEG_{22}$ were used as the outer shell [polymers: $PEI_{10500}(C_{18}mPEG_6)_{1.0}$, $PEI_{10500}(C_{18}mPEG_{10})_{1.0}$, $PEI_{10500}(C_{18}mPEG_{14})_{1.0}$, and $PEI_{10500}(C_{18}mPEG_{22})_{1.0}$]. In both series the hydrophobic inner shell consisted of the C_{18} alkyl chain. All polymers were easily soluble in water and chloroform.

The transport capacities were monitored for congo red as an example of polar guest molecules. As representative for nonpolar compounds nimodipine was chosen. The polymer concentration in the experiments was 1.00 g l^{-1} and 10 mg of drug/dye were used per 5 ml of polymer solution. After stirring for 24 h at r.t. the samples were filtrated and their absorbance was measured by UV/Vis spectroscopy. The obtained results are summarized in Table 6.

Table 6. Transport capacity (TC) and relative transport capacity (TC_{rel}) obtained by solid-liquid extraction for polymers with different PEI cores (M_n = 3600 and 10500 g mol^{-1}) functionalized with mPEGs of different lenght as an outer shell. The degree of functionalization was 0.7 for the PEI_{3600} core and 1.0 for the PEI_{10500} core. DF_A values were 0.4 and 0.45, respectively. The inner domain was in all cases the C_{18} alkyl chain.

Core[a] [g mol^{-1}]	Inner shell[b]	mPEG [unit][c]	M_n [g mol^{-1}] [d]	congo red		nimodipine	
				TC[e]	TC_{rel}[f]	TC[e]	TC_{rel}[f]
3600	C_{18}	6	18000	0.87	33.71	0.26	6.06
		10	22000	1.31	41.40	0.37	7.01
		14	26500	2.21	57.88	0.46	7.33
10500	C_{18}	6	58000	2.69	32.34	0.60	4.34
		10	73500	3.90	36.94	0.79	4.50
		14	95000	5.37	39.39	1.07	4.73
		22	125000	7.28	40.60	1.47	4.92

[a] M_n of PEI core; [b] length of the inner shell (carbon atoms); [c] length of the outer mPEG shell in glycol units, M_w of mPEG = 350, 550, 750, or 1100 g mol^{-1} for ~6, ~10, ~14, or ~22 units, respectively; [d] M_n = molecular weigth of core-multishell structure calculated from ^{1}H NMR spectrum; [e] transport capacity in mol_{guest} per mol_{host} ratio; [f] relative transport capacity in mg guest per g polymer; TC error is < 10 %.

The first series of measurements for polymers with PEI_{3600} core reveals an increase of both transport capacity and relative transport capacity for congo red and nimodipine, with a growing mPEG length (Figure 28). The increase was more significant for polar than for nonpolar guest molecules. The TC for congo red grows by a factor of 2.5 by changing the outer shell from $mPEG_6$ to $mPEG_{14}$. Also TC_{rel} for congo red increased by a factor of 1.7 by changing the shell length from ~6 to ~14 glycol units. In comparison to values obtained for congo red the changes of nimodipine encapsulation were mostly limited to TC, although an improvement of transport efficiency was still noticeable. Growth of the outer shell from $mPEG_6$ to $mPEG_{14}$ allows to encapsulate 1.8 times more of nimodipine molecules per polymer molecule. At the same time the relative transport capacity increase only and 21 %.

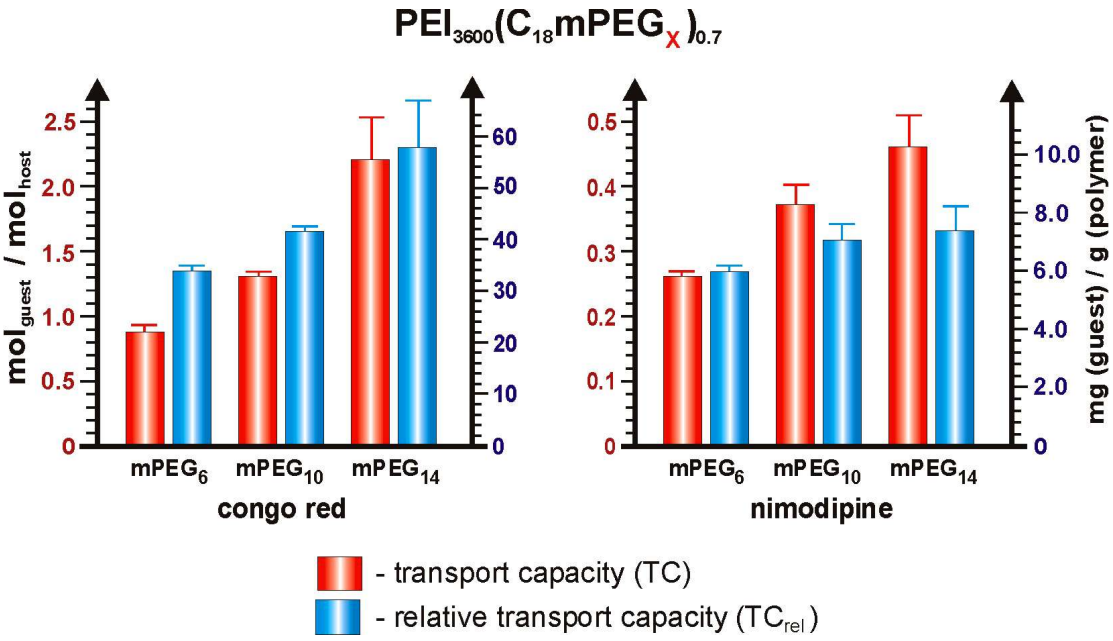

Figure 28. Influence of the length of the outer shell (~6, ~10, and ~14 glycol units) on the transport capacity (red columns, left scale) and relative transport capacity (blue columns, right scale) of core-multishell architectures with a PEI_{3600} core, C_{18} inner shell, and DF = 0.7 (DF_A = 0.45). **X** = average number of glycol units in the mPEG chains. Changes were determined by using congo red as a polar dye and nimodipine as nonpolar guest molecule.

The dependencies of the TC from the length of the poly(ethylene glycol) chain were confirmed with the results obtained for the series of polymers with PEI_{10500} core (Figure 29). The experiment was extended to four different sizes of the mPEG shell ($mPEG_6$, $mPEG_{10}$, $mPEG_{14}$, and $mPEG_{22}$). Similar to the results obtained for polymers with PEI_{3600} core, the transport capacity and relative transport capacity for polar and nonpolar molecules increased with increasing poly(ethylene glycol) chain length. For congo red the TC changed by a factor of approximately 1.4 (1.45; 1.38; 1.36) between neighboring polymers. For the polymers with $mPEG_6$ and $mPEG_{22}$ the encapsulation capacity grows by a factor of 2.7. The changes of the TC_{rel} were less pronounced but still noticable. With the increase of the mPEG length from ~6 to ~22 glycol units the enhancement of the congo red encapsulation efficiency by a factor of 1.3 was observed. Transport capacity for nimodipine also changes with increasing mPEG chain length. Similar to congo red the TCs for nimodipine increased by a factor of 1.4 (1.38, 1.35, 1.37) between neighboring polymers, however, TC_{rel} improved only by 0.6 mg per g (< 15 %).

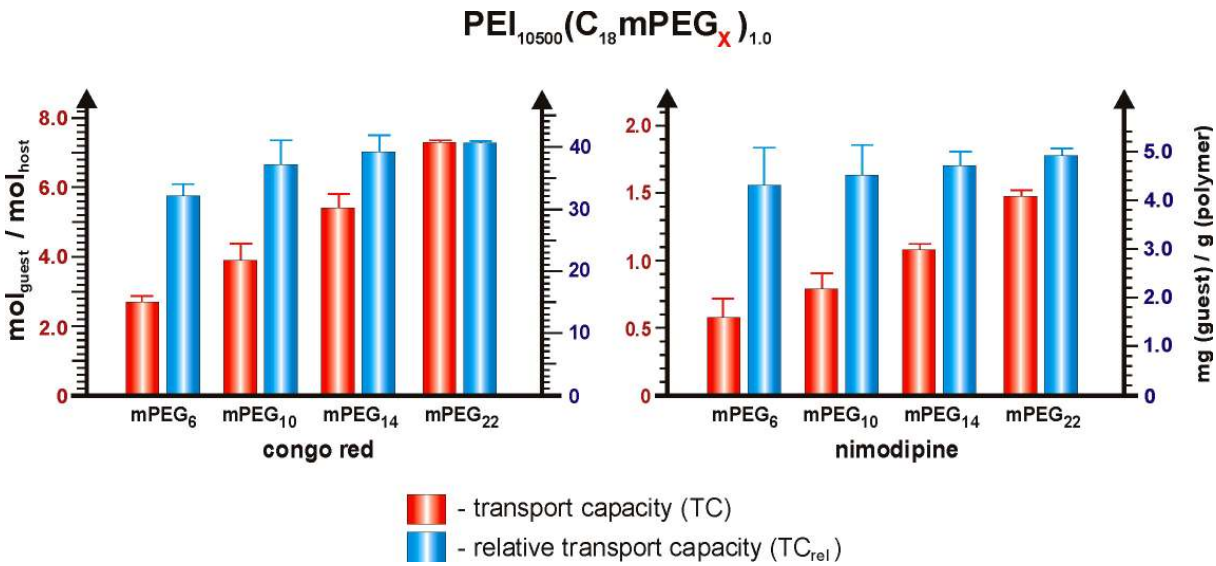

Figure 29. Influence of the size of the outer shell (~6, ~10, ~14, and ~22 glycol units) on the transport capacity (red columns, left scale) and relative transport capacity (blue columns, right scale) of core-multishell architectures with PEI_{10500} core, C_{18} inner shell, and DF = 1.0 (DF_A = 0.40). **X** = average number of glycol units in the mPEG chains. Changes were determined by using congo red as a polar dye and nimodipine as nonpolar guest molecule.

To summarize, the increase of the mPEG chain length led to an improvement of the transport abilities (TC and TC_{rel}) regardles of the guest molecules' polarity. This tendency is not dependent upon the core size and DF of the polymer. Thus the increase of the chain length has a larger influence on the transport efficiency of polymers with small core and/or lower DF. The best results for TC and TC_{rel} were obtained for the longest mPEGs – $mPEG_{14}$ and $mPEG_{22}$.

The influence of the poly(ethylene glycol) shell on the host-guest interactions leads to the conclusion that the outer shell is not only responsible for solubility properties but also plays an important role in the encapsulation process. This is in agreement with previous studies[57,350] where the influence of the mPEG chain length on the host-guest interactions of core-shell systems was discussed. In both publications the increase of the TC with growing mPGE chain length was confirmed and explained with the creation of additional cavities inside the polymeric structure suitable for guest molecules. The highest efficiency was found for a $mPEG_{40}$ shell.[350] Therefore the use of long mPEG chains as an outer shell in core-multishell architectures should be taken under consideration while designing new polymers.

3.4.4. Dependence of the TC on the length of the aliphatic chain

The dependency of the TC on the length of the aliphatic chain was determined with polymers containing two different cores (PEI_{3600} and PEI_{10500}) and three different alkyl chains lengths

(C_6, C_{12}, and C_{18}). The degree of functionalization was 0.9 (DF_A = 0.5 and DF_A = 0.4 for PEI_{3600} and PEI_{10500}, respectively) . As an outer shell $mPEG_6$ was used for all polymers. The TCs were tested by solid-liquid extraction with the standard procedure. The polymer concentration was 1.00 g l^{-1} and stirring time was 24 h. Results are summarized in Table 7.

Table 7. Transport capacity (TC) and relative transport capacity (TC_{rel}) obtained by solid-liquid extraction for polymers with two PEI cores (M_n = 3600 and 10500 g mol^{-1}) functionalized with different alkyl chains lengths (0, 6, 12, and 18 carbon atoms) as an inner shell. $mPEG_6$ was used as an outer shell for all polymers. The degree of functionalization was 0.9, DF_A = 0.5 (PEI_{3600}) and 0.4 (PEI_{10500}).

Core[a] [g mol^{-1}]	mPEG [unit][b]	Inner shell[c]	M_n [g mol^{-1}] [d]	congo red		nimodipine	
				TC[e]	TC_{rel}[f]	TC[e]	TC_{rel}[f]
3600	6	0	13000	0.02	0.85	0.00	0.00
		6	16500	0.65	26.80	0.09	2.26
		12	19000	0.94	34.44	0.30	6.57
		18	22500	1.54	47.20	0.44	8.24
10500	6	0	33000	0.53	11.14	0.00	0.00
		6	42000	1.63	27.02	0.25	2.45
		12	48500	2.55	36.58	0.53	4.58
		18	53500	5.21	67.86	0.67	5.24

[a] Molecular weigth of PEI core; [b] length of mPEG shell in glycol units; [c] length of the inner shell (carbon atoms) – C_0 = polymer contained only the mPEG shell; [d] M_n = molecular weight of core-multishell structure calculated from ^{1}H NMR spectrum; [e] transport capacity in mol_{guest} per mol_{host} ratio; [f] relative transport capacity in mg guest per g polymer; TC error is < 10 %.

The obtained result revealed an essential role of the aliphatic inner shell for the encapsulation of nonpolar molecules (Figure 30). No transport of nimodipine was observed in the absence of the nonpolar inner domain regardles of the core size. Nanotransporters with the shortest alkyl chain (C_6) show a very low TC and TC_{rel}. With increase of the length of the hydrophobic chain from C_6 to C_{18}, a significant improvement of the encapsulation capacity was detected. TC increased by a factor of 4.9 and 2.7 for polymers with PEI_{3600} and PEI_{10500} core, respectively. The TC_{rel} changed by a factor of 3.6 and 2.1, respectively. The results obtained for the C_{12} alkyl chain are located between the results for C_6 and C_{18}, although the major increase appeared for the inner shell growth from C_6 to C_{12} independent of the polymer core size. The prolongation of the alkyl chain from C_{12} to C_{18} still improved the TCs however the change is less pronounced.

The length (size) of the C_{12} chain and nimodipine is similar (13.7 and 14.7 Å, respectively) and therefore the best transport improvement might be obtained for chain lengths equal or greater than the encapsulated molecule. Prolongation of the alkyl chain allowed a further improvement of the encapsulation properties (TC and TC_{rel}), although it was less profitable.

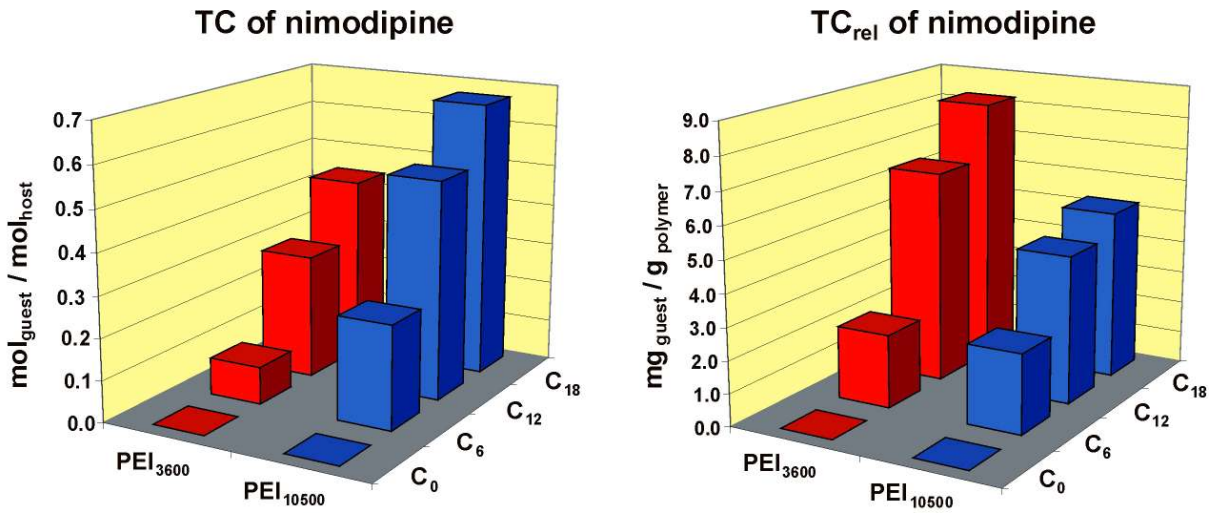

Figure 30. Transport capacity (left) and relative transport capacity (right) for nimodipine as an example of nonpolar guest molecules with $PEI_x(C_ymPEG_6)_{0.9}$ polymers where x = 3600 (red), 10500 (blue) and y = 0, 6, 12, 18. For clarity error bars are not shown. Error is typically below 10 %.

Surprisingly the inner nonpolar shell plays an important role in the transport of polar molecules (Figure 31). Since the positive influence of nonpolar domains on the transport of hydrophobic guest molecules was expected, a negative or passive interaction between polar molecules and the inner shell was assumed. In contrast to this expectation, a high positive effect was found.

Polymers without hydrophobic domain reveal basic transport capacities (TC) for polar molecules in the range of 0.02 and 0.53 for the polymers $PEI_{3600}(C_0mPEG_6)_{0.9}$ and $PEI_{10500}(C_0mPEG_6)_{0.9}$, respectively. With increasing inner shell size, the growth of the TC for congo red was observed for nanotransporters with both core sizes. The increase of TC for a polymer series with PEI_{3600} core was highest between C_0 and C_6. The change of the single-shell system into the multi-shell structure, even with the short C_6 alkyl chain, improved the TC by a factor of 32. The increase of the aliphatic chain length from C_0 to C_{18} improved the transport capacity by a factor of 77 (!). At the same time the TC_{rel} was improved by a factor of 55. The changes between $PEI_{10500}(C_0mPEG_6)_{0.9}$ and $PEI_{10500}(C_6mPEG_6)_{0.9}$ were smaller than obtained for the polymers with PEI_{3600} and were equal to a factor of 3.1 and 2.4 for TC and

TC_{rel}, respectively. With the increase of the inner shell from C_0 to C_{18} the transport capacity increase by 9.8 times.

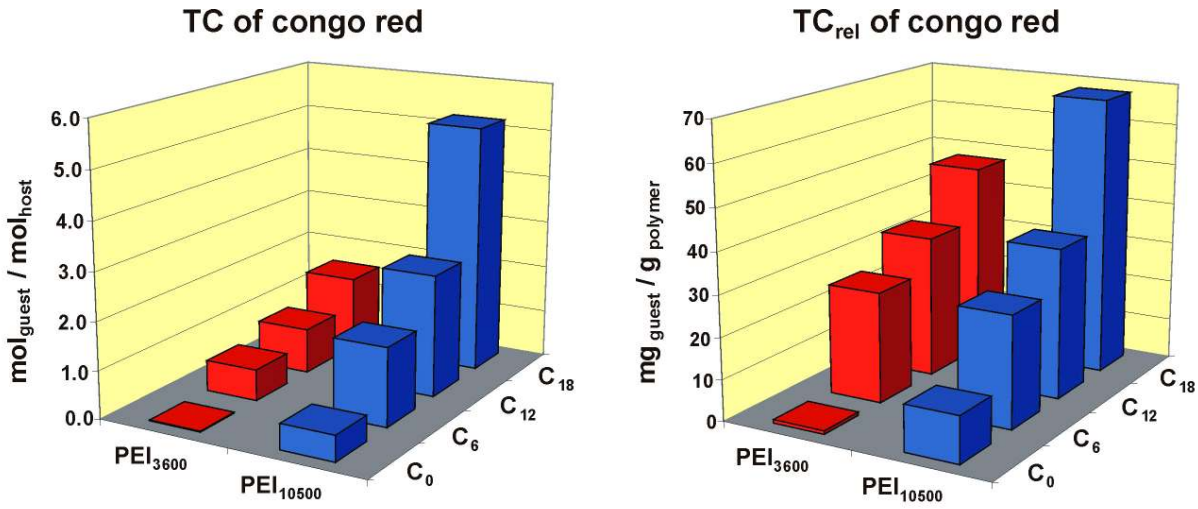

Figure 31. Transport capacity (left) and relative transport capacity (right) for congo red as an example of polar guest molecules with $PEI_x(C_ymPEG_6)_{0.9}$ polymers where x = 3600 (red), 10500 (blue) and y = 0, 6, 12, 18. For clarity reason error bars are not shown. Error is typical below 10 %.

Similar trends in TC changes with an increase of the inner shell length also have been observed for encapsulation of vitamin B_6 and β-carotene for the same series of polymers. For both types of guest molecules the maximum transport capacities were obtained for core-shell structures with C_{18} hydrophobic chain. No transport of nimodipine as well as vitamin B_6 was noticed for polymers without nonpolar domains and only limited transport for nanotransporters with C_6 inner domain.

In conclusion, the obtained results revealed an essential role of the inner hydrophobic shell for both polar and nonpolar molecules. The best results for TC and TC_{rel} were obtained for the longest aliphatic chain – C_{18} (1,18-octadecanodioic acid). Although the dependency of the transport of nonpolar molecules from the presence and length of an inner aliphatic domain can be explained, the strong possitive influence of hydrophobic chains on the encapsulation of polar molecules cannot be understood with the simple unimolecular transport model. In the case of nimodipine the inner shell probably creates special cavities with a nonpolar nanoenvironment that are suitable for the encapsulation of guest molecules. This mechanism, however, cannot explain the enhancement of the transport of polar molecules. The addition of hydrophobic chains to the polymeric structure should cause a decrease of the TC for congo red and vitamin B_6 due to a lower total polymer hydrophilicity. Such behavior was observed for increasing DF which will be described in chapter 3.4.5. Meanwhile, the transport capacity increases systematically with the prolongation of the inner shell up to TC values which are almost 10 times (!) better than for polymers without nonpolar

domain. To explain this phenomenon a new model of supramolecular aggregation of nanotransporters was created, confirmed experimentally, and described in detail in chapter 6. In general it was assumed that core-multishell architectures do not act as unimolecular transporters (liposome-like polymers) but create a supramolecular non-covalently bound structure *via* self-assembly which is responsible for the encapsulation phenomenon. Since the presence of long aliphatic chains in the polymeric structure enhances the transport efficiency, the inner domain must play an important role in the self-assembly process or/and stabilization of the aggregates.

3.4.5. Dependence of the TC on the degree of functionalization (DF) of the core

To fully understand the structure-transport capacity dependency of the nanotransporters the influence of the degree of functionalization on the encapsulation properties was determined. A polymer series of $PEI_{3600}(C_{18}mPEG_6)_x$ with x = 0.3, 0.5, 0.7, 0.9 was chosen for the test. The encapsulation experiments were performed *via* solid-liquid extraction method with the standard procedure described in chapter 3.4. The concentration of all polymers were 1.00 g l^{-1}. As guest molecules nimodipine and vitamin B_6 were selected. The obtained results reveal a very strong TC dependency for both types of guest molecules (Table 8).

Table 8. Transport dependency from the degree of functionalization of the core for polymers $PEI_{3600}(C_{18}mPEG_6)_x$, x = 0.3, 0.5, 0.7, 0.9.

Polymer	M_n [g mol^{-1}] [a]	DF [b]	vitamin B_6		nimodipine	
			TC[c]	TC_{rel}[d]	TC[c]	TC_{rel}[d]
$PEI_{3600}(C_{18}mPEG_6)_{0.3}$	9500	0.3	5.92	128.84	0.09	4.03
$PEI_{3600}(C_{18}mPEG_6)_{0.5}$	14000	0.5	2.21	32.41	0.17	4.99
$PEI_{3600}(C_{18}mPEG_6)_{0.7}$	18000	0.7	1.61	18.35	0.26	6.06
$PEI_{3600}(C_{18}mPEG_6)_{0.9}$	22500	0.9	1.04	11.89	0.44	8.24

Core M_n = 3600 g mol^{-1}; inner shell = C_{18} and outer shell = $mPEG_6$; [a] M_n = molecular weight of core-multishell architecture calculated from ^{1}H NMR spectrum; [b] degree of functionalization of the core calculated from ^{1}H NMR spectrum; [c] transport capacity in mol_{guest} per mol_{host} ratio; [d] relative transport capacity in mg guest per g polymer; TC error is < 10 %.

The transport capacities of nimodipine and vitamin B_6 reveal a contradictive behavior upon change of the DF (Figure 32). The TC for polar molecules decreases with increasing core functionalization while the encapsulation capacity for nonpolar guest grows at the same time. The maximum of the transport capacity of vitamin B_6 was obtained for polymers with the lowest DF of 0.3. The same polymer showed a minimal encapsulation ratio for

nimodipine. The TC for polymers with the highest degree of functionalization (DF = 0.9) revealed a decrease of the transport of polar molecules by a factor of 5.7 and an increase of the encapsulation of nonpolar guests by 4.9 times. The relative transport capacity for vitamin B_6 decreased 10.8 times and TC_{rel} increased for nimodipine by a factor of 2.1.

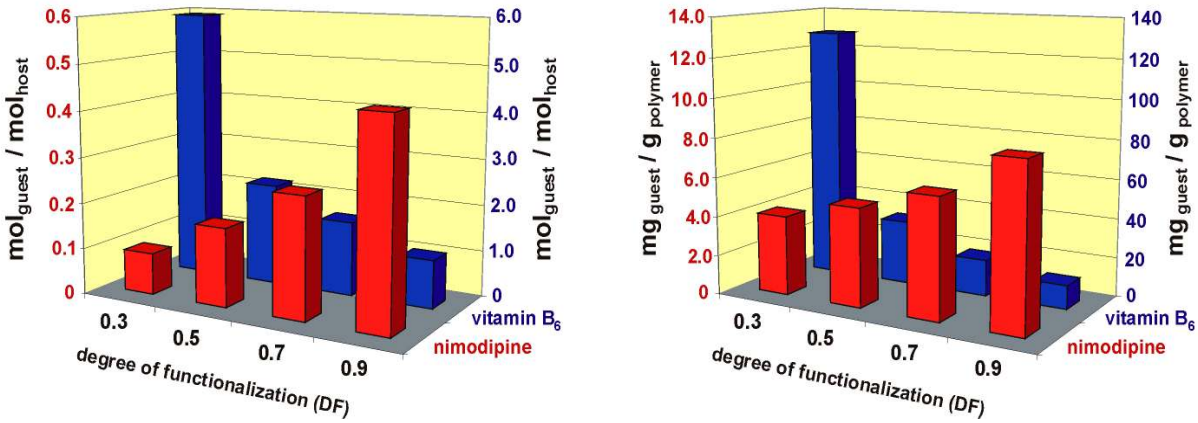

Figure 32. Influence of the degree of functionalization (DF) on the transport capacity (left) and relative transport capacity (right) for nimodipine (red, left scale) and vitamin B_6 (blue, right scale). Experiments were performed for a series of polymers $PEI_{3600}(C_{18}mPEG_6)_x$ with x = 0.3, 0.5, 0.7, 0.9.

The observed behavior can be explained by the change of the polarity of the core-multishell architecture upon modification of the DF of the core. The increase of the DF introduces more amphiphilic chains into the polymer structure (increase from 9 to 28 chains for DF change from 0.3 to 0.9 for PEI_{3600} core, respectively). Thus the percentage of the part of nonpolar chains per g of polymer also increases. For the polymer with a DF of 0.3 and PEI_{3600} core the hydrophobic domain shares ~27.5 %, outer mPEG shell shares ~32.5 %, and PEI core shares ~40.0 % of the polymer mass. With increasing DF up to 0.9 the mass distribution changes to ~38.5% for the inner shell, ~45.0 % for outer one, and only ~16.5 % of mass fall on the core. Additionally, the functionalization of the core with amphiphilic chains convert the polar amino groups into the less polar amide bonds. This causes a strong decrease in the core polarity and thus also might influence the TC for guest molecules. To confirm this theory, the polymer $PEI_{3600}(C_{18}mPEG_{10})_{0.5}$ was modified *via* reaction with acetic acid anhydride. This reaction converts free primary and secondary amino groups of PEI_{3600} into acetoamide groups which simulates a polarity of the core of polymer with DF > 1.0 but with a number of amphiphilic chains equal to the number of chains in $PEI_{3600}(C_{18}mPEG_{10})_{0.5}$. The transport capacity of the obtained $PEI_{3600}(C_{18}mPEG_{10})_{0.5}Ac$ polymer was determined for nimodipine and vitamin B_6. Encapsulation experiments revealed a decrease of the TC for polar guest molecules by a factor of 2.8 and an increase of the TC for nonpolar ones by a

factor of 1.8. The observed changes are in very good agreement with the expectations. Thus it can be concluded that the polarity of the polymer core and the polymer in general possesses a significant influence on transport capacity. Increasing polarity has a positive influence on the TC for polar guest molecules and a negative one on the transport of nonpolar guest molecules.

3.4.6. Dependence of the TC on the concentration of the polymer

TC measurements of the dilution series of various core-multishell architectures were performed. Solid-liquid extraction experiments were made with polymer concentrations ranging from 3.125×10^{-3} to 1.00 g l^{-1} in water and chloroform for nonpolar and polar guest molecules. With every dilution the concentration changed by a factor of two. As model compounds congo red, nimodipine, nile red, and β-carotene were chosen. Polymers with two different PEI cores (PEI_{3600} and PEI_{10500}), and three different outer mPEG shell ($mPEG_6$, $mPEG_{14}$, and $mPEG_{22}$) with DF values of 0.7 and 1.0 were selected. In all cases the alkyl C_{18} chain was used as the inner nonpolar domain.

The transport capacity - polymer concentration dependency for polar guest molecules was determined with congo red. Tests were performed in chloroform with $PEI_{3600}(C_{18}mPEG_6)_{0.6}$, $PEI_{3600}(C_{18}mPEG_6)_{0.7}$, $PEI_{10500}(C_{18}mPEG_{14})_{1.0}$, and $PEI_{10500}(C_{18}mPEG_{22})_{1.0}$ (Table 9, Figure 33). All experiments revealed a very similar encapsulation behavior. Independent of the differences between polymers, the transport of guest molecules only occurred above a concentration of core-shell architecture of approximately 0.10 g l^{-1}. An exception was the $PEI_{10500}(C_{18}mPEG_{22})_{1.0}$ with a threshold concentration at 0.05 g l^{-1}. Below the mentioned concentration no encapsulation of congo red was observed. The transport of guest molecules appeared suddenly at the concentration of 0.10 g l^{-1} and very high n_{guest}/n_{host} ratios (TC) were obtained. The most significant change in the transport capacity was observed for $PEI_{10500}(C_{18}mPEG_{14})_{1.0}$ where the value increased from 0 at a concentration of 0.05 g l^{-1} (5.26×10^{-7} M) to 12.6 for concentration of 0.10 g l^{-1} ($10{,}52 \times 10^{-7}$ M). This is the highest transport value obtained for this polymer. For all polymers the highest transport values were achieved at threshold point. The further increase of the polymer concentration caused a decrease of transport capacity. For example, the congo red encapsulation for $PEI_{10500}(C_{18}mPEG_{22})_{1.0}$ dropped from the maximum of 14.7 molecules per polymer to only 7.3 guest molecules when concentration of the polymer increased from 0.10 g l^{-1} to 0.80 g l^{-1}. The TC of congo red for $PEI_{10500}(C_{18}mPEG_{14})_{1.0}$ decreased by a factor of 2.34 for the same concentration change. Core-shell nanotransporters with PEI_{3600} revealed a similar trend in transport capacity changes with increasing polymer concentration. The encapsulation of the dye could be directly observed

by the accompanying color change of the chloroform phase (insert in Figure 33). It is noteworthy that the relative transport capacities almost had the same values which cannot be easily deduced from the Figure 33 (Table 9). Three out of four tested polymers ($PEI_{3600}(C_{18}mPEG_6)_{0.7}$, $PEI_{10500}(C_{18}mPEG_{14})_{1.0}$, and $PEI_{10500}(C_{18}mPEG_{22})_{1.0}$) revealed a maximum encapsulation efficiency in approximately 85 mg dye per g polymer (87.98, 92.16, 81.81 mg per g, respectively) at polymer concentrations of 0.10 g l^{-1} and than transport decreasing to a level of 30 – 40 mg per g with increasing polymer concentration up to the 1.00 g l^{-1}. Only $PEI_{3600}(C_{18}mPEG_6)_{0.6}$ revealed much higher maximum TC_{rel}, although this value was obtained at a higher concentration and the drop of TC (and TC_{rel}) by 1.5 times was less pronounced than for the other core-shell architectures. At higher polymer concentrations (above 0.80 g l^{-1}) a slow stabilization of the TC could be observed for all tested macromolecules.

It is worth mentioning that the error of TC for all tested nanotransporters was the always highest at the threshold concentration. For the others samples the error significantly decreased, usually below 5%. This suggests a high instability of the system (aggregates) at the critical encapsulation point.

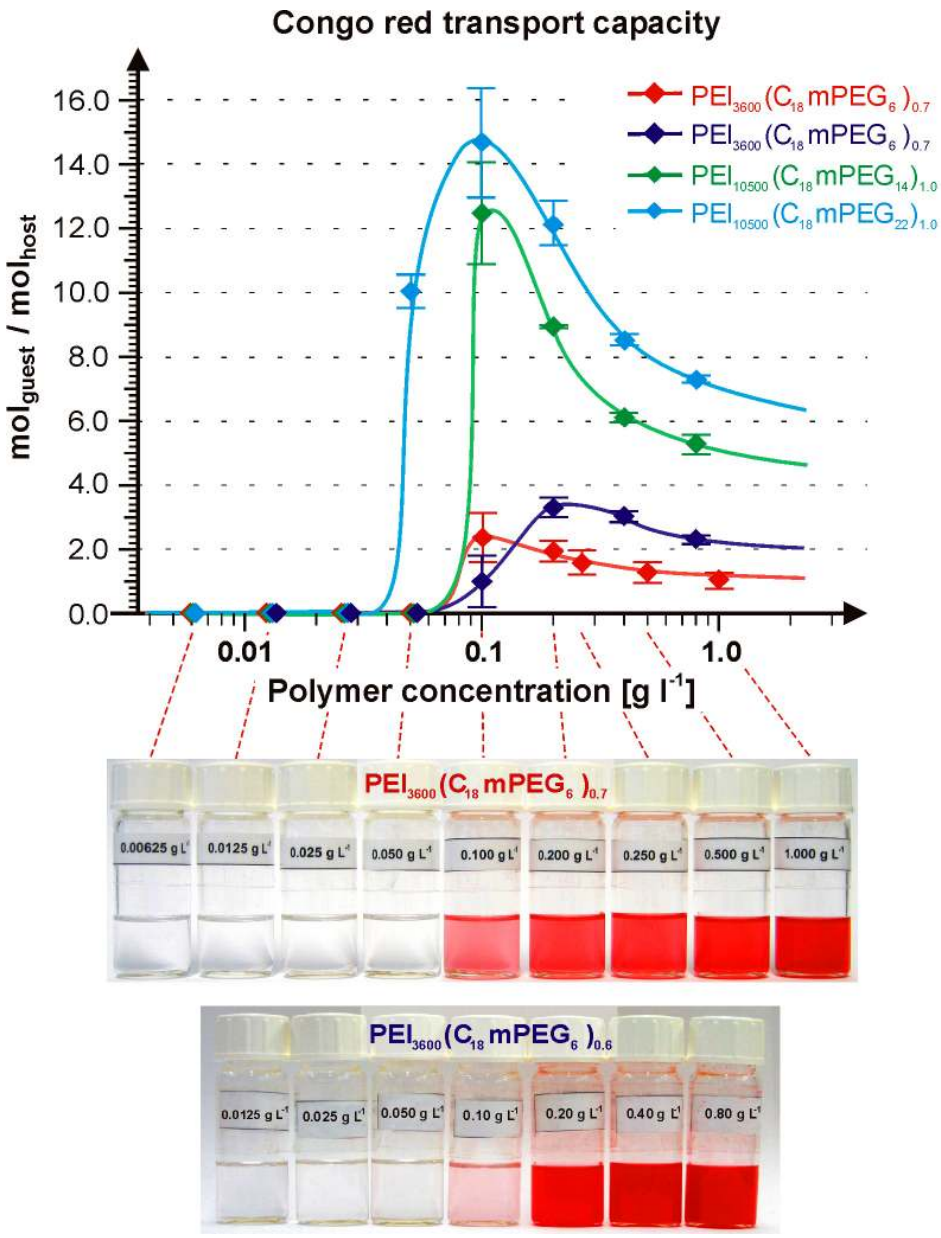

Figure 33. Influence of the polymer concentration on the transport capacity (TC) of $PEI_{3600}(C_{18}mPEG_6)_{0.6}$ (♦), $PEI_{3600}(C_{18}mPEG_6)_{0.7}$ (♦), $PEI_{10500}(C_{18}mPEG_{14})_{1.0}$ (♦), and $PEI_{10500}(C_{18}mPEG_{14})_{1.0}$ (♦) for congo red in chloroform. The inserts visualize the congo red transport for different polymer concentrations with increasing concentration from left to right. Top insert - $PEI_{3600}(C_{18}mPEG_6)_{0.7}$; bottom insert - $PEI_{3600}(C_{18}mPEG_6)_{0.6}$.

Table 9. Congo red transport dependency from polymer concentration.

Polymer concentration[a] [g l^{-1}]	Polymer name							
	$PEI_{3600}(C_{18}mPEG_6)_{0.6}$ M_n[b] = 16000		$PEI_{3600}(C_{18}mPEG_6)_{0.7}$ M_n[b] = 18000		$PEI_{10500}(C_{18}mPEG_{14})_{1.0}$ M_n[b] = 95000		$PEI_{10500}(C_{18}mPEG_{14})_{1.0}$ M_n[b] = 125000	
	TC[c]	TC_{rel}[d]	TC[c]	TC_{rel}[d]	TC[c]	TC_{rel}[d]	TC[c]	TC_{rel}[d]
0.00625	-	-	-	-	-	-	-	-
0.0125	-	-	-	-	-	-	-	-
0.025	-	-	-	-	-	-	-	-
0.05	-	-	-	-	-	-	10.03	55.92
0.10	1.09	47.48	2.27	87.98	12.57	92.16	14.68	81.81
0.20	3.37	146.54	1.56	60.36	8.95	65.60	12.09	67.38
0.25			1.26	44.75				
0.40	3.02	131.51			6.12	44.91	8.52	47.49
0.50			1.08	41.83				
0.80	2.31	100.46			5.37	39.39	7.28	40.59
1.00			0.87	33.73				

[a] Polymer concentration in the organic phase in g l^{-1}; [b] M_n = molecular weight of core-multishell architecture calculated from ^{1}H NMR spectrum [g mol^{-1}]; [c] transport capacity in mol_{guest} per mol_{host} ratio; [d] relative transport capacity in mg guest per g polymer; TC error ranged between 10 % for the samples with a polymer concentration equal or higher than 0.20 g l^{-1} and up to 25 % for samples with the concentration of 0.10 g l^{-1}.

Studies on the TC dependency from the polymer concentration for nonpolar molecules were performed with three different nonpolar guest molecules: nimodipine, β-carotene, and nile red. Polymer $PEI_{3600}(C_{18}mPEG_6)_{0.7}$ was chosen for the tests. Additionally $PEI_{10500}(C_{18}mPEG_{14})_{1.0}$ was tested in a dilution series with β-carotene as a comparison (Figure 34). The result revealed similar trends for the TC as obtained for congo red. Below a threshold concentration of 0.05 – 0.10 g l^{-1} no host-guest interactions between polymer and dye/drug molecules were observed. At the critical concentration, encapsulation capacity for all tested nonpolar guest molecules reached almost immediately the highest values. With the further increase of the polymer concentration the TC of $PEI_{3600}(C_{18}mPEG_6)_{0.7}$ for nimodipine and nile red decreased by a factor of 2.8 (nimodipine) and 3.2 (nile red). Also samples with

β-carotene showed a transport drop at higher concentrations for both tested polymers, although the changes were less intensive (approximately 25 %). Like in the case of polar guest molecules, experiments with nonpolar compounds revealed slow stabilization and smaller errors of the TC values at polymer concentrations higher than 0.80 g l^{-1}.

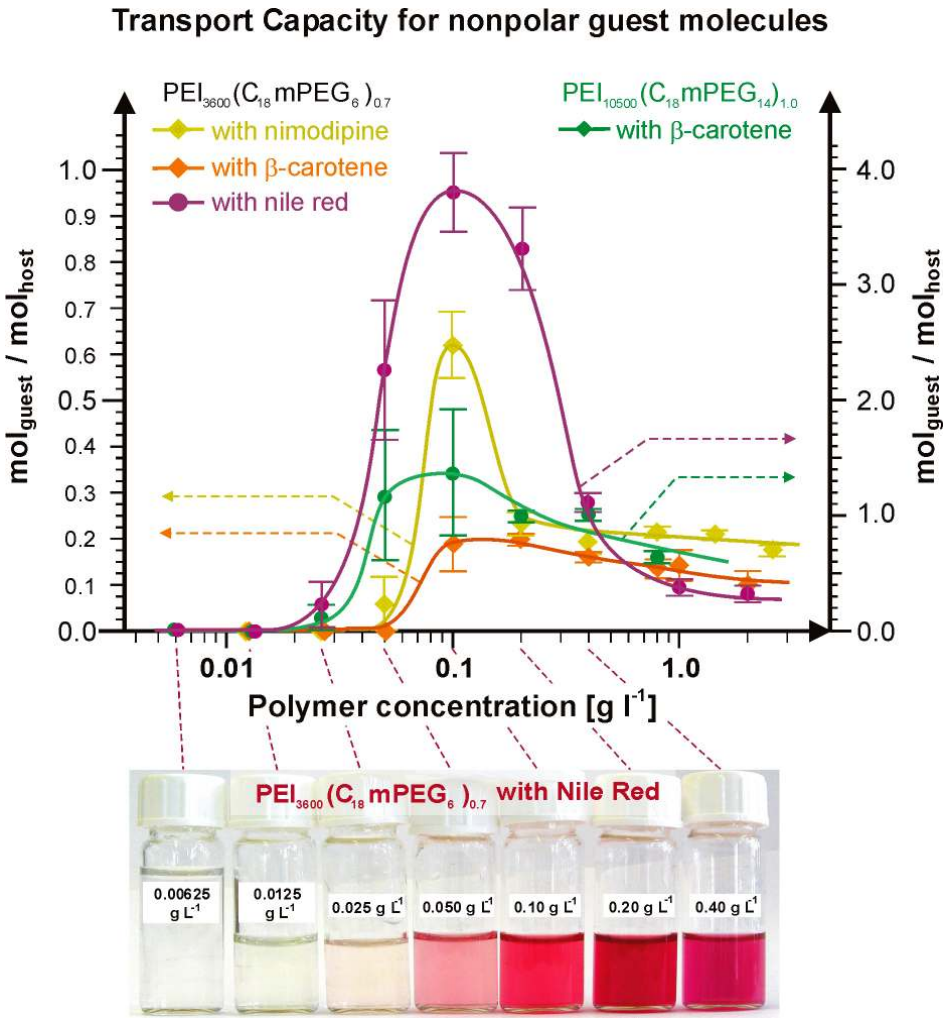

Figure 34. Influence of the polymer concentration on the transport capacity (TC) of $PEI_{3600}(C_{18}mPEG_6)_{0.7}$ for nimodipine (♦, left scale), β-carotene (♦, left scale), and nile red (♦, right scale) in water. TC of $PEI_{10500}(C_{18}mPEG_{14})_{1.0}$ for β-carotene (♦, right scale) is also shown on the graph. The insert visualizes the nile red transport for $PEI_{3600}(C_{18}mPEG_6)_{0.7}$ polymer with increasing concentration from left to right.

To summarize, independent of the polarity and structure of the guest molecules a non-linear transport capacity-polymer concentration dependency was observed. At concentrations of nanotransporter in the range of 0.00625 – 0.025 g l^{-1} no encapsulation of dye or drug molecules was observed. At concentrations above approximately 0.80 g l^{-1} stable, slowly decreasing transport capacity values were observed. In the region between concentrations of 0.05 to 0.40 g l^{-1} two important phenomena were observed. The first was a

sudden appearance of host-guest interactions between dye/drug and polymer. By changing the nanotransporters content in solution by a factor of two, the transport of congo red rapidly increased from zero to 12 dye molecules per host. For nonpolar molecules the changes in TC were usually lower, and the TC increase was up to a maximum of 2.5 molecules per polymer. This is due to the generally smaller TC values for hydrophobic guest molecules. Therefore the changes can still be described as significant. It is noteworthy that for all polymers the initial concentration where transport occurred was located between 0.05 and 0.10 g l^{-1} independent of the molecular weight of polymers. Thus the molar concentrations of the nanotransporters were significantly different. For example, the concentration where congo red was encapsulated was equal to 5.56×10^{-6} M for $PEI_{3600}(C_{18}mPEG_6)_{0.7}$ and 1.05×10^{-6} M for $PEI_{10500}(C_{18}mPEG_{14})_{1.0}$. Second, all experiments revealed that after a fast initial growth of the TC, a further increase of the polymer concentration resulted in a rapid decrease of the transport capacity. The rate of decrease was specific and depended on the guest molecules and polymer. In general, the higher (intensive) initial growth was followed by a more rapid drop of the TC. Therefore all curves possess a maximum TC at the beginning of the encapsulation area. After the initial TC peak a stabilization of the encapsulation efficiency was observed for all experiments. It is important to mention that the measurement error was not constant and changed with the concentration. At the critical transport point the differences between the measured transport capacities were about 25 – 30 % while the errors for higher polymer concentrations were below 10 %.

The described non-linear changes of the TC with linear modifications of polymer concentration indicates that the transport of guest molecules only appears when a micellization or aggregation of a core-multishell architectures takes place. A self-assembled aggregation was also suggested earlier to explain the influence of the inner shell on the TC for polar molecules (chapter 3.4.4.). This stands in contrast to the unimolecular transport model reported previously for core-shell architectures.[19,73,75,80,356,361]

The critical nanotransporter concentration in which encapsulation of guest molecules is possible is very similar to the critical micelle concentration (CMC) observed for low molecular weight surfactants[234] and diblock copolymers.[235-239] The rapid appearance of the transport capacity of core-multishell nanotransporters is comparable to a situation when amphiphilic molecules organize themselves into a supramolecular structure (micelle) which allows them to encapsulate guest molecules. Further analyses of the transport phenomenon were performed with AFM and CryoTEM microscopy and by dynamic light scattering (DLS) (described in chapter 6) and revealed different than micellar type of self-organization. Therefore, in analogy to the CMC the discussed threshold concentration of polymer will be named critical aggregation concentration (CAC).

Similar to diblock copolymer micelles, core-multishell architectures reveal a very slow break up of the aggregates after dilution below the CAC (see chapter 1.5.2. and Figure 11).[237] The stability of the aggregates below the critical concentration was determined by diluting a $PEI_{3600}(C_{18}mPEG_6)_{0.7}$ polymer solution in $CHCl_3$ with encapsulated congo red. The initial concentration of the solution was 0.10 g l^{-1}. Then the sample was divided and the resulting sub-samples were diluted 4, 8, 16, 32, and 64 times by addition of an adequate volume of pure chloroform. After 48 h the absorbance of all solutions was measured by UV/Vis spectroscopy (Figure 35). For a better comparison, spectra of diluted samples were intensified by the dilution factor. All tests revealed the presence of encapsulated congo red in the chloroform solution. The absorbances of samples were approximately 20 % lower than for the original solution, although no correlation between the dilution factor and the drop of absorbance was found. Therefore it can be assumed that the decrease of the signal intensity results not only from the break up of aggregates but also from experimental errors (inaccuracy in dilution and UV/Vis spectrometer error). Nevertheless, the results confirmed the long time stability of the aggregates below the CAC concentration even after dilution by a factor of 64 (from 5.56×10^{-6} M to 8.69×10^{-8} M).

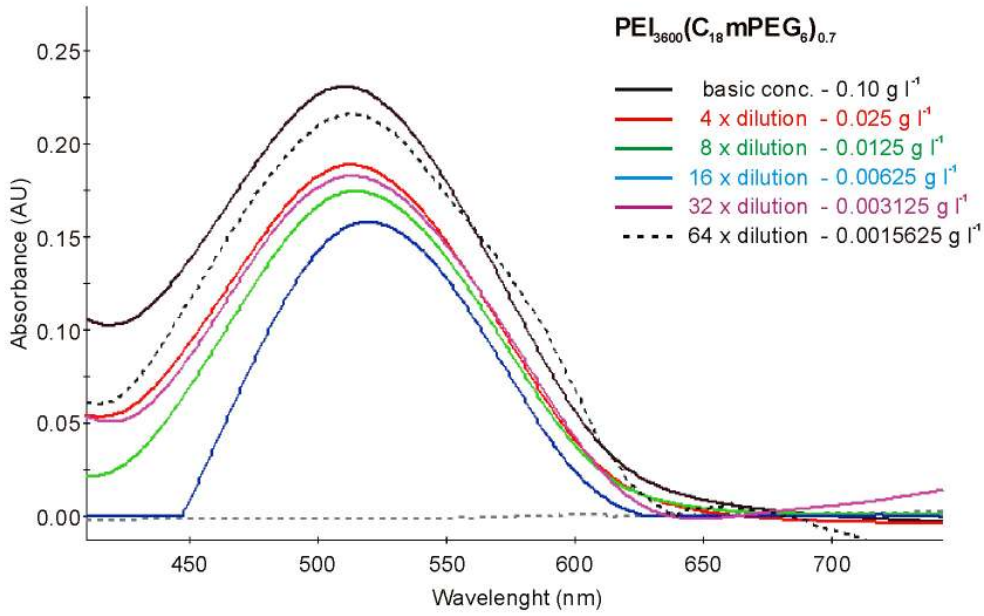

Figure 35. The UV/Vis spectra of $PEI_{3600}(C_{18}mPEG_6)_{0.7}$ with encapsulated congo red (λ_{max} = 512 nm) above (black solid line) and below the CAC of 0.10 g l^{-1}. The series was obtained by dilution of the initial sample by factors of 4, 8, 16, 32, and 64; UV/Vis absorbance was measured after 48 h. The dashed grey line shows the absorbance of the polymer at a concentration of 0.05 g l^{-1} after the encapsulation experiment with congo red. No presence of the dye can be noticed. All spectra were intensified to obtaine the theoretical concentration of polymer in samples equal to 0.10 g l^{-1}.

3.4.7. The dynamics of the encapsulation process by core-multishell architectures

The observed differences of the transport capacities obtained via solid-liquid extraction and liquid-liquid extraction (chapter 4.3.1.), as well as the discovery of a polymer aggregation encapsulation mechanism open the question about the dynamics of the uptake process of guest molecules.

The first test was performed for $PEI_{3600}(C_{18}mPEG_6)_{0.7}$ and with congo red as the polar guest molecule. A chloroform solution of the polymer with a concentration of 0.5 g l^{-1} (2.78×10^{-5} M) was divided into 32 identical samples, 4 ml each, and 20 mg of solid dye was added to every phial. The congo red suspensions in polymer solution were stirred at r.t. on a magnetic stirrer with 1000 rpm. With time the samples were removed one by one from the stirrer, filtrated, and the absorbance was measured by UV/Vis spectroscopy. The obtained transport capacities were plotted as a function of time (Figure 36). A very fast encapsulation process was reveal. The 25 % of the maximum transport capacity (TC_{max}) of the polymer was achieved within the first minute of experiment. After 15 minutes approximately 45 % of TC_{max} was obtained. At this point the uptake of congo red by the nanotransporters (aggregates) slowed down but was still significant. Within 2 h $PEI_{3600}(C_{18}mPEG_6)_{0.7}$ reached its highest loading point (TC_{max}). Further stirring of the samples (up to 24 h) did not improve the TC, although fluctuations of the ratio were observed. Due to the much higher transport capacities obtained by liquid-liquid extraction the experiment was performed for an additional 48 h to prove that the highest loading of the polymer had been achieved. Samples collected after 48, 72, and 96 h after the beginning of the experiment revealed an unexpected drop of the transport capacity. Except for a solution with the ratio of n_{host} / n_{guest} equal to approximately 0.72 (dark red color of chloroform phase) all solutions after filtration were colorless. UV/Vis measurements confirmed a very low concentration of the dye in the range of 0.02 – 0.03 guest molecules per polymer. ^{1}H NMR studies revealed a strong decrease of the polymer concentration (drop of signal intensity) in the solution in comparison to the original sample (before encapsulation). Therefore it can be assumed that polymer precipitated during the encapsulation process after stirring for a longer time. The repetition of the experiment was performed for different polymers ($PEI_{3600}(C_{18}mPEG_{10})_{0.7}$ and $PEI_{10500}(C_{18}mPEG_6)_{0.7}$) and confirmed the previous observations.

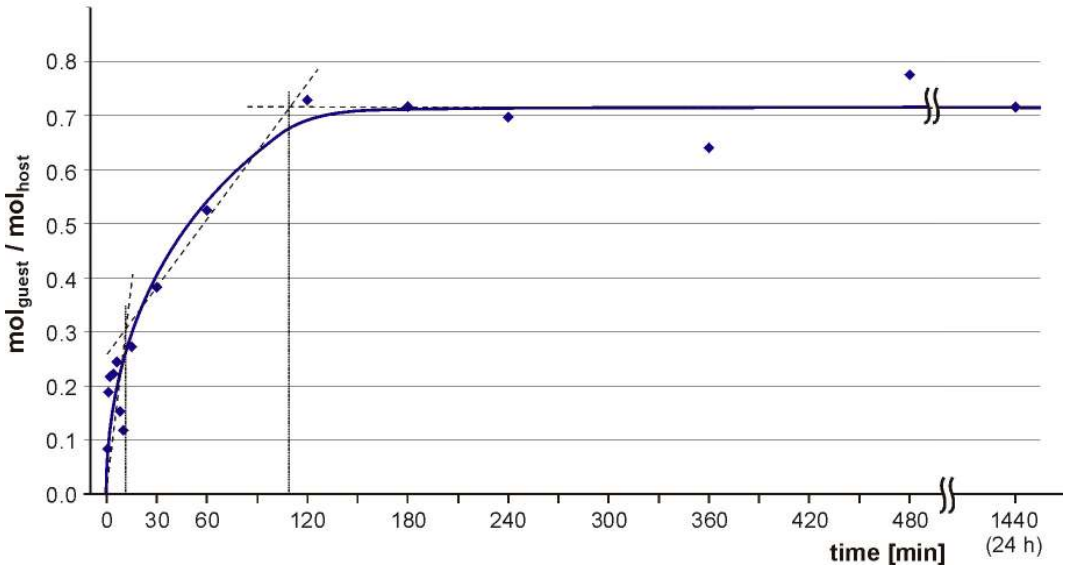

Figure 36. The dynamics of congo red encapsulation by $PEI_{3600}(C_{18}mPEG_6)_{0.7}$. Concentration of polymer = 0.5 g l^{-1} (2.78×10^{-5} M). 4.0 ml of polymer solution and 20 mg of dye was used for the solid-liquid extraction method.

For a better understanding of the encapsulation process and precipitation of the polymer from the solution, experiments with the $PEI_{10500}(C_{18}mPEG_6)_{0.7}$ nanotransporter were performed due to the higher stability of this system and higher values of transport capacity. Experiments were prepared as previously described with a polymer concentration of 0.5 g l^{-1} (1.14×10^{-5} M) in chloroform. The stock solution was divided into 4 ml portions and the samples were segregated into five groups. To every group a different amount of solid dye was added – 2, 10, 20, 50, and 100 mg per phial, respectively. The encapsulation dynamics for the first 2 h of the experiments were similar to the one obtained for $PEI_{3600}(C_{18}mPEG_6)_{0.7}$. In this time period TC rose very quickly and the growth was proportional to the amount of added solid congo red. After this initial rapid growth a slow stabilization of the transport capacity was observed. Although, in contrast to the core-multishell architecture with the PEI_{3600} core, the TC did not stabilize on one level but slowly increased further with time (Figure 37). After 24 h the loading of the polymer was determined to 1.75, 5.04, 7.22, 8.61, and 6.55 congo red molecules per polymer for samples stirred with 2, 10, 20, 50, and 100 mg of dye, respectively. This gives a nearly linear dependency between the encapsulation efficiency and the amount of added solid congo red for the first three points. The improvement of the TC for 50 mg sample was lower than expected but the addition of bigger amoutn of solid material still had a positive influence on the encapsulation efficiency. Surprisingly, the addition of 100 mg of dye resulted in a lower transport capacity than addition of 20 or 50 mg of congo red.

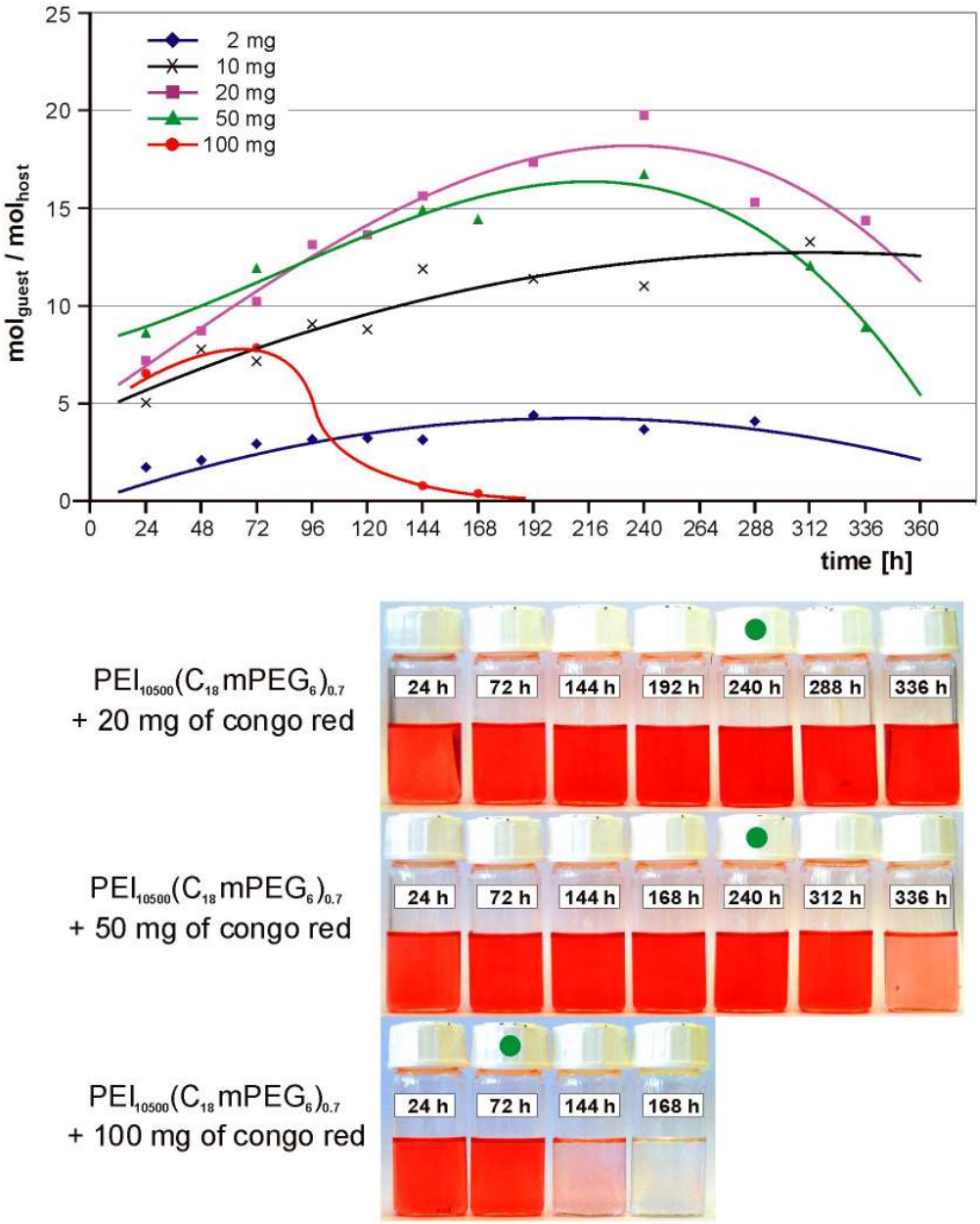

Figure 37. The dynamics of the encapsulation of congo red in $PEI_{10500}(C_{18}mPEG_6)_{0.7}$ with different amounts of solid congo red. 4 ml of polymer solution and 2, 10, 20, 50, and 100 mg of solid dye were used for solid-liquid extraction method. Concentration of polymer = 0.5 g l^{-1} (1.14×10^{-5} M). Error is below 10 %. The inserts visualize the congo red transport for $PEI_{10500}(C_{18}mPEG_6)_{0.7}$ stirred with 20, 50, and 100 mg of solid dye. Samples with the highest TC at every series are marked with a green dot. All samples were diluted five times with chloroform to obtain a better contrast.

The experiment also revealed that an increase of the encapsulation (stirring) time can optimize the TC even up to the value of 20 (!) congo red molecules per single polymer. This is equal to approximately 300 mg of dye per one gram of polymer (Figure 37). Thus the transport capacity obtained by solid-liquid extraction exceeded the value obtained for liquid-liquid extraction method (TC = 14.7, chapter 3.4.1).

The dynamics of the congo red uptake in the time period 24 – 336 h (1 – 14 days) was strongly dependent upon the amount of solid dye added to the polymer solution. With only 2 mg of congo red an initial fast growth of encapsulation capacity in the first 24 h experiment was observed. Then a slow, nearly constant increase of TC took place in the following 4 days. At this time the TC value increased from 1.8 (24 h) to 3.2 (96 h), which represents an improvement of the guest-host molar ratio by 1.8 times (average increase by 0.48 guest molecule per polymer daily). After 8 days of stirring the transport achieved the highest for the 2 mg series ratio equal to 4.4 congo red molecules per polymer. After more than 192 h (8 days) of stirring all observed TC values were lower than 4.4. This can be treated as a stabilization or regression of the transport efficiency due to precipitation of the polymer. This behavior was similar for the samples mixed with 10 mg of congo red. Initial increase of the TC to the level of 5.1 after 24 h was followed by a growth of the transport capacity by a factor of 1.8 after 96 h (increase of TC by 1.3 per day). The increase factors between TCs measured after 24 h and 96 h were identical for both (2 mg and 10 mg congo red additions) experiments. Further growth of the TC with time was observed up to the level of 13.3 after 13 days. No clear maximum of saturation point of the polymer with the dye was detected.

The most interesting results were obtained for samples with the 20 and 50 mg of solid dye. In both cases a high loading of the polymer was observed after 24 h, although only a small difference between the samples with 20 and 50 mg was noticed. In contrast to the experiments with 2 and 10 mg of congo red, where the encapsulation ratio grew faster for samples with a bigger amount of dye, the suspension with 20 mg of solid material allowed a faster loading of the polymer than the suspension with 50 mg. For the first 6 days the TC increased almost linearly, daily by 1.7 and 1.3 guest molecules per nanotransporter for 20 and 50 mg samples, respectively (The transport capacities for both experimentals obtained an identical value after approximately 103 h of stirring.) Further proceeding of the tests led to a clear maximum of the transport capacities after approximately 10 days for both experiments. The TC values were equal to 19.8 for samples with 20 mg and 16.7 with 50 mg of congo red (TC_{rel} = 313 and 269 mg per gram, respectively). After this time a clear decrease of the transport capacity for both series was observed (inserts at Figure 37, mostly visible for $PEI_{10500}(C_{18}mPEG_6)_{0.7}$ with 50 mg of dye after 366 h of stirring). This is due to an overloading of the polymer with dye. Overloaded aggregate become unstable by probably further accumulation with other supramolecular species which cause precipitation of the core-multishell architectures from the solution.

In the experiment with an addition of 100 mg of congo red the oversaturation (overloading) phenomenon was detected much earlier. After 24 h the transport capacity was lower from the ones for the series of 20 mg and 50 mg, which was unlike the previously

observed trends. After another 48 h only small (>30 %) improvement of the TC was noticed. Continuation of the encapsulation procedure led to the drop of dye concentration in the solution to the value of 0.8 molecule per polymer (9.8 times) after 6 days. Stirring for additional 24 h resulted in a further decrease of the TC by a factor of 2 to the level of 0.4. At this point the sample after filtration was colorless and the presence of the congo red in the chloroform phase was only confirmed by UV/Vis spectroscopy (bottom insert at Figure 37).

From the experiments presented above, it can be concluded that the encapsulation of polar guest molecules during the solid-liquid extraction occurs in two separate steps. At the first stage, a very fast uptake of congo red into the aggregated structure (of approximately 10 guests per host daily) can be observed in the first 2 to 4 h of the experiment. At the second stadium of encapsulation, the dye uptake clearly slows down by order of magnitude (increase by around one dye molecule per polymer per day). Stirring of the samples for 10 days led to an increase of the TC by two to three times in comparison to the samples stirred for 24 h. At this stage the amount of solid material in the mixture and the duration of the experiment plays a crucial role for the whole process. For the best encapsulation efficiency the optimal dose of guest molecules has to be found. Not enough or too much of the material will lead to lower than the maximal possible transport capacity values. It can be assumed that the dynamics of the encapsulation can be presented as a function of the contact surface between dye and polymer. A higher area of the contact surface leads to a faster phase transfer. A limiting factor is the instability of the polymer-dye complexes. In contrast to liquid-liquid extraction where water probably act as a phase-transfer catalyst and prevents the overloading of the polymer, solid-liquid transfer does not stop at maximal loading point. The aggregates become unstable, accumulates further between each other and, as a consequence, precipitate. On the one hand, this allows better transport capacities. For example, TC of 19.8 and TC of 14.7 was reached for the same polymer by solid-liquid and liquid-liquid extraction, respectively. On the other hand too long an encapsulation process results in a drop of the TC. Unfortunately the results obtained for congo red cannot be generalized for all other possible guest molecules. Although tests with vitamin B_6 confirmed the presented tendencies and time dependencies, the values gained for rose bengal revealed a precipitation of the polymer with the addition of more than 2 mg of solid dye after 24 h (Figure 38). Differences in the polymer composition also have an influence on the optimal loading time and guest molecules amount. For example, TC of $PEI_{3600}(C_{18}mPEG_6)_{0.7}$ and 10 mg of congo red corresponds to the behavior of $PEI_{10500}(C_{18}mPEG_6)_{0.7}$ with 100 mg of solid dye.

The most important fact is that all samples were stable after filtration for at least six months and no precipitation from the solution was observed. This was also true for the

highest loaded sample of $PEI_{10500}(C_{18}mPEG_6)_{0.7}$ with 20 mg of congo red after 240 h of stirring.

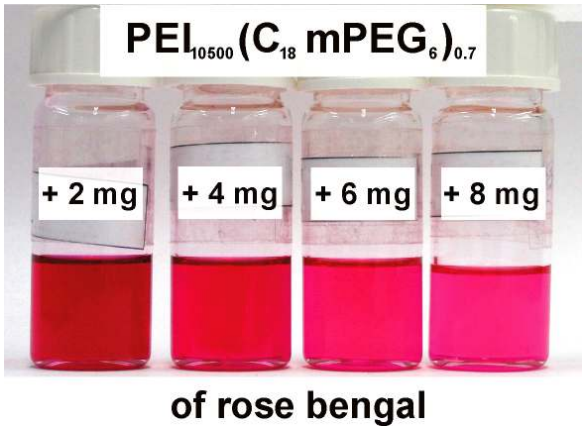

Figure 38. The transport capacity of $PEI_{105000}(C_{18}mPEG_6)_{0.7}$ for rose bengal obtained by addition of 2, 4, 6, and 8 mg of solid dye to 4 ml of the polymer solution in $CHCl_3$ (concentration 0.5 g l^{-1}; 1.14×10^{-5} M). Samples were stirred for 24 h at r.t. and filtrated *via* 0.45 μm filter. The color change from dark red (left) to light magenta (right) indicates the decrease of the TC. This is due to precipitation of the polymer as a result of the oversaturation of polymer with the dye.

The dynamics of the encapsulation of nonpolar guest molecules was determined with a nile red. The obtained dependency presented a similar behavior compared to the results with congo red (Figure 39). A very fast growth of the TC value was observed for the first hour. After that the encapsulation slowed down and almost constant growth was observed for the next 6 days. No maximum of transport capacity was found after 7 days of experiment, although 14 days after filtration a precipitate was observed at the bottom of the sample with the highest TC. This is in contrast to the observations made for congo red.

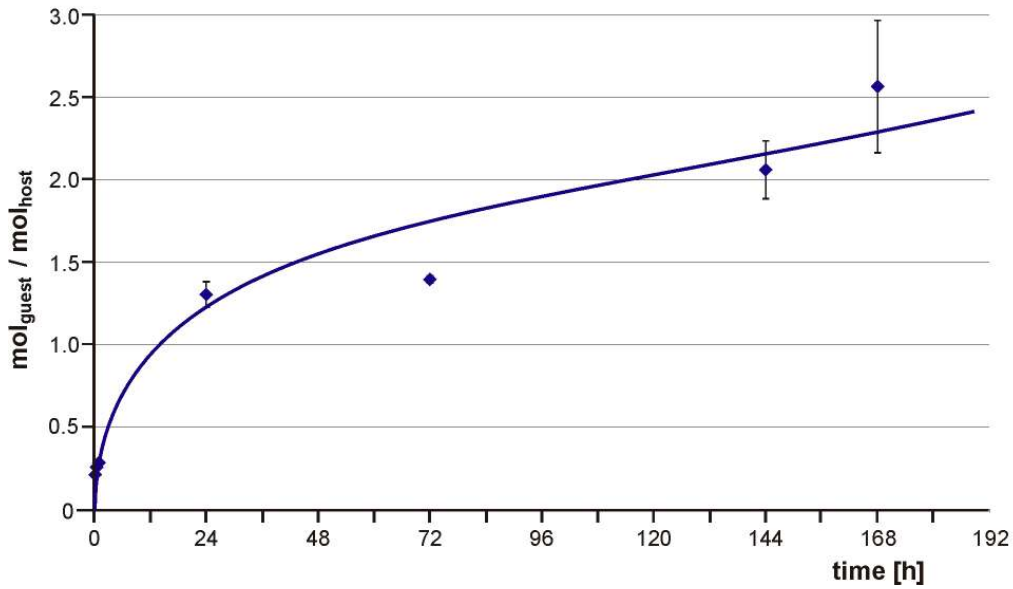

Figure 39. The dynamics of nile red encapsulation by $PEI_{10500}(C_{18}mPEG_6)_{0.7}$. Concentration of polymer = 0.5 g l^{-1} (1.14×10^{-5} M). 4.0 ml of polymer solution and 5 mg of dye were used in the solid-liquid extraction method.

During the experiment, changes in λ_{max} and the shape of the absorption spectrum of nile red were observed. This was a result of a polarity change in the nanoenvironment around the dye molecules and will be discussed in chapter 6 of this work.

3.4.8. Summary and discussion of the transport capacity

The universal transport abilities and transport efficiency of core-multishell architectures were determined by using several polar and nonpolar molecules: congo red, rose bengal, vitamin B_6, β-carotene, nimodipine, and nile red for broad matrix spectrum.

The influence of every domain of the polymer: core, inner shell, and outer shell as well as the core functionalization level (shells density) on the TCs was established to optimize the transport capacity. Additionally, the dependencies on the polymer concentration, the amount of solid guest molecules in the solution, and the time of the experiment were tested and presented. Due to the solubility of the polymers in the aqueous as well as in the organic phase, the solid-liquid extraction method was used for the determination of transport capacity to avoid the diffusion of the polymer between the phases. Additionally the liquid-liquid extraction method was not possible for nonpolar guest molecules which eliminates this method for hydrophobic guest encapsulation.

The influence of the core size on the TC was tested with two different PEI cores with M_n equal to 3600 and 10500 g mol^{-1}. The results reveal a significant improvement of the transport capacitiy up to 5 times for polar and 2 times for nonpolar guest molecules for polymers with bigger core. This was in agreement with the observations previously reported

for other core-shell architectures.[75,87,356,361] Although the TC increases for both polar and nonpolar molecules, only the relative transport capacity for polar molecules profits from increasing core size. The improvement in the TC for hydrophobic guests was not significant enough to counterbalance the change of the molecular weight of the polymer. This results in a drop of the TC_{rel} of the nanotransporters for tested nonpolar guests. Therefore, polymers designed for the encapsulation of polar molecules should be based on the large hyperbranched PEI core, while core-multishell architectures for the transport of nonpolar guests should contain cores with the smaller molecular weight. The described dependency has to be considered during the design of new nanotransport systems.

The influence of the outer shell consisting of mPEG chains upon the transport capacity is in agreement with the observations reported by Kojima[57] and Yang.[350] Increasing mPEG chain length results in the improvement of the TC independent of the guest molecules' polarity and size. This is possibly due to the fact that poly(ethylene glycol) chains can create additional complex sites inside the polymer structure which act as additional encapsulation sites.[350] Therefore the best TC results were obtained for the longest used polyether chains – $mPEG_{22}$. The creation of special nanocompartments for guest molecules becomes especially important if self-aggregation is the reason for the host-guest ability of the polymer. Intermolecular interactions between polymer allows the creation of not only intramolecular complex sites but also compartments located at the contact surface between nanotransporters. Although the increase of the transport capacities were significant – by a factor of two or more – the improvement of the TC_{rel} was rather limited to polymers with smaller cores (increase by approximately 50% between $mPEG_6$ and $mPEG_{14}$). For polymers with the PEI_{10500} core TC_{rel} increased usually by 10 – 20 % ($mPEG_6$ to $mPEG_{14}$). Nevertheless, for the optimization of the polymer loading and the higher biocompatibility the use of longer mPEG chains ($mPEG_{14}$, $mPEG_{22}$) is recommended.

Transport capacity measurements also revealed the crucial role of the inner shell in the core-multishell systems for their encapsulation ability. Polymers without a hydrophobic domain were highly limited in encapsulation of polar and could not encapsulate nonpolar guest molecules. In this situation the creation of cavities with special nanoenvironments for the encapsulation of guest molecules cannot be the only explanation for this transport phenomenon. In the case of nonpolar molecules the formation of nanocompartments with a nonpolar environment is definitely one of the driving forces for guest uptake and will be discussed in chapter 6. However, for polar molecules this explanation is not satisfying. The creation of nonpolar compartments should effect in a decrease of the TC due to a reduction of the polarity of the polymer. Such a polarity change was described in the literature and led to repulsive interactions between host and guests.[75,78,81,82] In the case of core-multishell nanotransporters, with a growing inner domain from C_0 to C_{18}, the transport capacity

increased by a factor of 10 and 77 for polymers with PEI_{10500} and PEI_{3600} as a core, respectively. Therefore it can be assumed that additionally to the creation of nonpolar nanocompartments, the inner shell acts as a stabilizer of the polymeric aggregates which are responsible for the transport of polar and nonpolar molecules.

In contrast to the unexpected influence of the inner shell on the nanotransporters TC, changes of the polymer polarity caused by different degree of functionalization (DF) predictably affect the encapsulation abilities. As was demonstrated on core-shell systems with dendritic PPI core by Baars[75] and Pistolis,[78] the decrease of the polymer polarity resulted in an improvement of nonpolar molecules transport. The TC for polar molecules decreased with the polarity drop. In practice core-multishell architectures for transport of polar molecular should possess a low DF while polymers designed for nonpolar molecules should possess a high DF. Also the modification of the amino groups of the core into the amides *via* the amidation with acetic anhydride results in similar changes of the transport capacities of nanotransporters, i.e., for nonpolar guest molecules.

In addition to the above reported structure-transport capacity dependencies, other external factors such as the presence of the water, polymer concentration, amount of guest molecules, and time of encapsulation significantly influence the TC of core-multishell architectures.

The experiments performed at various polymer concentrations revealed a nonlinear transport capacity for all tested guest molecules due to the aggregation of polymers. This behavior was also reported by Krämer[361] for core-shell architectures with PEI cores and aliphatic chains as a shell. However, only an increase of the transport capacity with dilution of the polymer was noticed. For core-multishell architectures micellar-like type of encapsulation was observed with a clear critical aggregation concentration (CAC) similar to the critical micelle concentration (CMC).[235-239] Below the threshold point no host-guest interactions were observed. At the critical concentration all tested polymers disclosed a maximum of the transport capacity. This might be due to the optimal polymer-guest “packing” in the aggregate. Further increase of the polymer concentration led to a decrease of the TC. Above a certain concentration (usually 1.0 g l^{-1}), the TC stabilizes and becomes constant. It is noteworthy that the aggregates remained stable for several days after dilution below the CAC which is characteristic for diblock polymeric micelles.[237]

Other important factors influencing the transport capacity of polymers are the time of the encapsulation process and the amount of the solid guest molecules added to the polymer solutions. Solid-liquid extraction experiments performed with changing both factors revealed their large influence on the transport capacities. It can be concluded that the TC is a function of the contact surface between polymer and guest molecules and the time of the interactions. The detailed dynamics of the phase transfer are characteristic for the type of guest

molecules as well as the type of the polymer. Therefore encapsulation optimization tests should be performed for every compound of interest. However, the general tendencies of the encapsulation behavior can be used to design experiments and to interpretate the results. The most important fact is the possibility of overloading the polymer with guest molecules by a too long encapsulation process. This led to the precipitation of nanotransporters probably due to the further uncontrolled aggregation, and resulted in an overall decrease of the transport efficiency.

Despite of all optimization experiments performed for the core-multishell architectures, the highest TC values obtained for congo red were significantly different from others described in the literature. Transport capacities in the range of 50 molecules of rose bengal[75] or 100 (!) molecules of congo red[361] per polymer were reported (these TCs were obtained with the liquid-liquid extraction method). This is equal to the value of 2.5 g of dye per gram of polymer. Furthermore, it was stated that every tertiary amine group of a PAMAM dendrimer can bind one guest molecule.[19] These calculations would suggest a transport capacity at the level of 150 guest molecules per polymer with PEI_{10500} core for only secondary and tertiary amine groups. However, it was also reported that only up to 10 molecules – depending on their size – were encapsulated in the “Dendritic Box”.[71,72] Also about 26 methotrexate molecules were encapsulated by mPEG modified [G4]-PAMAM dendrimer.[57] The best transport result obtained for $PEI_{10500}(C_{18}mPEG_6)_{0.7}$ nanotransporters was about 20 congo red molecules per host (~0.3 g per gram). This is in strong contrast to the results obtained by Baars[75] or Krämer.[361] The results obtained for methotrexate [57] as a nonpolar molecule are also not comparable to the transport capacities of core-multishell systems where a maximum of 5 guest molecules per host could be encapsulated. This is probably due to the different model of encapsulation where the crucial role of transport is reserved for supramolecular aggregates and no unimolecular transport is taken under consideration.